Title
Reflective Cracking Study: First-Level Report on the HVS Rutting Experiment

Authors
Jones, David
Harvey, John T
Steven, B.

Publication Date
2008-10-01

Peer reviewed

April 2007
Research Report: UCPRC-RR-2007-06

Reflective Cracking Study: First-Level Report on the HVS Rutting Experiment

Authors:
B. Steven, D. Jones and J. Harvey

Partnered Pavement Research Program (PPRC) Contract Strategic Plan Element 4.10:
Development of Improved Rehabilitation Designs for Reflective Cracking

PREPARED FOR:

California Department of Transportation
Division of Research and Innovation
Office of Roadway Research

PREPARED BY:

University of California
Pavement Research Center
UC Davis, UC Berkeley

DOCUMENT RETRIEVAL PAGE		Research Report: UCPRC-RR-2007-06
Title: Reflective Cracking Study: First-Level Report on the HVS Rutting Experiment		
Authors: B. Steven, D. Jones and J. Harvey		
Prepared for: Caltrans	**FHWA No:** CA091073H	**Date**: April 2007
Contract No: 65A0172	**Client Reference No:** SPE 4.10	**Status:** Stage 6, Approved Version

Abstract:

This report is the seventh in a series of first-level analysis reports that describe the results of HVS testing on a full-scale experiment being performed at the Richmond Field Station (RFS) to validate Caltrans overlay strategies for the rehabilitation of cracked asphalt concrete. It describes the results of the six HVS rutting testing sections, designated 580RF through 585RF, carried out on six different overlays. The test forms part of Partnered Pavement Research Center Strategic Plan Element 4.10: "Development of Improved Rehabilitation Designs for Reflective Cracking."

HVS trafficking on the first section (582RF) commenced on September 4, 2003 and was completed on the last section (583RF) on December 16, 2003. A temperature chamber was used to maintain the pavement temperature at 50°C±4°C. A dual tire (720 kPa pressure) and a channelized, unidirectional 60 kN loading configuration was used. Load repetitions to failure (12.5 mm) on each of the sections varied between 726 and 8,266. Findings and observations based on the data collected during this HVS study include:

- The majority of the rutting occurred in the underlying DGAC layer.
- The rutting was fairly uniform along the length of each test section.
- Little or no deformation was measured in the base and subgrade materials.

The ranking of rutting performance (keeping in mind that most damage occurred in the underlying DGAC layer) based on the number of repetitions to reach an average maximum rut depth of 12.5 mm, from best to worst was:

1. 90-mm AR4000-D (8,266 repetitions)
2. 45-mm MB4-G (3,043 repetitions)
3. 45-mm RAC-G (2,324 repetitions)
4. 90-mm MB4-G (1,522 repetitions)
5. 45-mm MB15-G (914 repetitions)
6. 45-mm MAC15-G (726 repetitions)

No recommendations as to the use of the modified binders in overlay mixes are made at this time. These recommendations will be included in the second-level analysis report, which will be prepared and submitted on completion of all HVS and laboratory testing.

Keywords:
Reflective cracking, overlay, modified binder, HVS test, rutting test, MB Road

Related documents:
UCPRC-RR-2005-03, RR-2006-04, RR-2006-05, RR-2006-06, RR-2006-07, RR-2006-12, RR-2007-05

Signatures:

B. Steven 1st Author	J Harvey Technical Review	D. Spinner Editor	J. Harvey Principal Investigator	M Samadian Caltrans Contract Manager

DISCLAIMER

The contents of this report reflect the views of the authors who are responsible for the facts and accuracy of the data presented herein. The contents do not necessarily reflect the official views or policies of the State of California or the Federal Highway Administration. This report does not constitute a standard, specification, or regulation.

PROJECT OBJECTIVES

The objective of this project is to develop improved rehabilitation designs for reflective cracking for California.

This objective will be met after completion of four tasks identified by the Caltrans/Industry Rubber Asphalt Concrete Task Group (RACTG):

1. Develop improved mechanistic models of reflective cracking in California
2. Calibrate and verify these models using laboratory and HVS testing
3. Evaluate the most effective strategies for reflective cracking
4. Provide recommendations for reflective cracking strategies

This document is one of a series addressing Tasks 2 and 3.

ACKNOWLEDGEMENTS

The University of California Pavement Research Center acknowledges the assistance of the Rubber Pavements Association, Valero Energy Corporation, and Paramount Petroleum which contributed funds and asphalt binders for the construction of the Heavy Vehicle Simulator test track discussed in this study.

REFLECTIVE CRACKING STUDY REPORTS

The reports prepared during the reflective cracking study document data from construction, Heavy Vehicle Simulator (HVS) tests, laboratory tests, and subsequent analyses. These include a series of first- and second-level analysis reports and two summary reports. On completion of the study this suite of documents will include:

1. Reflective Cracking Study: Summary of Construction Activities, Phase 1 HVS testing and Overlay Construction (UCPRC-RR-2005-03).
2. Reflective Cracking Study: First-level Report on the HVS Rutting Experiment (UCPRC-RR-2007-06).
3. Reflective Cracking Study: First-level Report on HVS Testing on Section 590RF — 90 mm MB4-G Overlay (UCPRC-RR-2006-04).
4. Reflective Cracking Study: First-level Report on HVS Testing on Section 589RF — 45 mm MB4-G Overlay (UCPRC-RR-2006-05).
5. Reflective Cracking Study: First-level Report on HVS Testing on Section 587RF — 45 mm RAC-G Overlay (UCPRC-RR-2006-06).
6. Reflective Cracking Study: First-level Report on HVS Testing on Section 588RF — 90 mm AR4000-D Overlay (UCPRC-RR-2006-07).
7. Reflective Cracking Study: First-level Report on HVS Testing on Section 586RF — 45 mm MB15-G Overlay (UCPRC-RR-2006-12).
8. Reflective Cracking Study: First-level Report on HVS Testing on Section 591RF — 45 mm MAC15-G Overlay (UCPRC-RR-2007-04).
9. Reflective Cracking Study: HVS Test Section Forensic Report (UCPRC-RR-2007-05).
10. Reflective Cracking Study: First-level Report on Laboratory Fatigue Testing (UCPRC-RR-2006-08).
11. Reflective Cracking Study: First-level Report on Laboratory Shear Testing (UCPRC-RR-2006-11).
12. Reflective Cracking Study: Backcalculation of FWD Data from HVS Test Sections (UCPRC-RR-2007-08).
13. Reflective Cracking Study: Second-level Analysis Report (UCPRC-RR-2007-09).
14. Reflective Cracking Study: Summary Report (UCPRC-SR-2007-01). Detailed summary report.
15. Reflective Cracking Study: Summary Report (UCPRC-SR-2007-03). Four-page summary report.

CONVERSION FACTORS

SI* (MODERN METRIC) CONVERSION FACTORS				
APPROXIMATE CONVERSIONS TO SI UNITS				
Symbol	**Convert From**	**Multiply By**	**Convert To**	**Symbol**
LENGTH				
in	inches	25.4	millimeters	mm
ft	feet	0.305	meters	m
AREA				
in^2	square inches	645.2	square millimeters	mm^2
ft^2	square feet	0.093	square meters	m2
VOLUME				
ft^3	cubic feet	0.028	cubic meters	m^3
MASS				
lb	pounds	0.454	kilograms	kg
TEMPERATURE (exact degrees)				
°F	Fahrenheit	5 (F-32)/9 or (F-32)/1.8	Celsius	C
FORCE and PRESSURE or STRESS				
lbf	poundforce	4.45	newtons	N
lbf/in^2	poundforce/square inch	6.89	kilopascals	kPa
APPROXIMATE CONVERSIONS FROM SI UNITS				
Symbol	**Convert From**	**Multiply By**	**Convert To**	**Symbol**
LENGTH				
mm	millimeters	0.039	inches	in
m	meters	3.28	feet	ft
AREA				
mm^2	square millimeters	0.0016	square inches	in^2
m^2	square meters	10.764	square feet	ft^2
VOLUME				
m^3	cubic meters	35.314	cubic feet	ft^3
MASS				
kg	kilograms	2.202	pounds	lb
TEMPERATURE (exact degrees)				
C	Celsius	1.8C+32	Fahrenheit	F
FORCE and PRESSURE or STRESS				
N	newtons	0.225	poundforce	lbf
kPa	kilopascals	0.145	poundforce/square inch	lbf/in^2

*SI is the symbol for the International System of Units. Appropriate rounding should be made to comply with Section 4 of ASTM E380. (Revised March 2003)

EXECUTIVE SUMMARY

This report is the seventh in a series of first-level analysis reports that describe the results of HVS testing on a full-scale experiment being performed at the Richmond Field Station (RFS) to validate Caltrans overlay strategies for the rehabilitation of cracked asphalt concrete. It describes the results of the HVS rutting tests, designated 580RF through 585RF, carried out on the following overlays:

- Section 580RF: Half-thickness (45-mm) MB4 gap-graded overlay with minimum 15 percent recycled tire rubber (referred to as "MB15-G" in this report);
- Section 581RF: Half-thickness (45-mm) rubberized asphalt concrete gap-graded overlay (RAC-G), included as a control for performance comparison purposes;
- Section 582RF: Full-thickness (90-mm) AR4000 dense-graded asphalt concrete (AR4000-D) overlay, included as a control for performance comparison purposes;
- Section 583RF: Half-thickness (45-mm) MB4 gap-graded overlay (referred to as "45 mm MB4-G" in this report);
- Section 584RF: Full-thickness (90-mm) MB4 gap-graded overlay (referred to as "90 mm MB4-G" in this report), and
- Section 585RF: Half-thickness (45-mm) MAC15TR gap-graded overlay with minimum 15 percent recycled tire rubber (referred to as "MAC15-G" in this report).

The testing forms part of Partnered Pavement Research Center Strategic Plan Element 4.10: "Development of Improved Rehabilitation Designs for Reflective Cracking." The objective of this project is to develop improved rehabilitation designs for reflective cracking for California. This objective will be met after completion of the following four tasks:

1. Develop improved mechanistic models of reflective cracking in California
2. Calibrate and verify these models using laboratory and HVS testing
3. Evaluate the most effective strategies for reflective cracking
4. Provide recommendations for reflective cracking strategies

This report is one of a series addressing Tasks 2 and 3. It consists of three main chapters. Chapter 2 provides information on the experiment layout, pavement instrumentation and monitoring methods, pavement design, and the test details, including test duration, loading program, test section failure criteria, and the environmental conditions recorded over the duration of the test. Chapter 3 summarizes the data collected and includes discussion of air and pavement temperatures during testing (measured with thermocouples), permanent deformation (measured on the surface with the Laser Profilometer and at

depth with Multi-depth Deflectometers), and visual inspections. Chapter 4 provides a summary and lists key findings.

The underlying pavement was designed following standard Caltrans procedures and it incorporates a 410-mm (16 in) Class 2 aggregate base on subgrade with a 90-mm (3.6 in) dense-graded asphalt concrete (DGAC) surface. Design thickness was based on a subgrade R-value of 5 and a Traffic Index of 7 (~121,000 equivalent standard axles, or ESALs). The thickness for the AR4000-D overlay was determined according to Caltrans Test Method 356. The other overlay thicknesses were either the same or half of the AR4000-D overlay thickness. Details on construction and the first phase of trafficking are provided in an earlier report.

Laboratory fatigue and shear studies are being conducted in parallel with HVS testing. Results of these studies will be detailed in separate reports. Comparison of the laboratory and test section performance will be discussed in a second-level report once the data from the studies have been collected and analyzed.

HVS trafficking on the sections commenced on September 4, 2003, and was completed on December 16, 2003. During this period, the following load repetitions were applied on each section with a 60 kN (13,500 lb) load, using a dual tire (720 kPa [104 psi] pressure) and a channelized, unidirectional loading configuration. A temperature chamber maintained the pavement temperature at 50°C±4°C (122°F±7°F).

- 580RF (45-mm MB15-G): 2,000 repetitions, equating to 10,980 thousand ESALs
- 581RF (45-mm RAC-G): 7,600 repetitions, equating to 41,725 thousand ESALs
- 582RF (90-mm AR4000-D): 18,564 repetitions, equating to 101,919 thousand ESALs
- 583RF (45-mm MB4-G): 15,000 repetitions, equating to 82,352 thousand ESALs
- 584RF (90-mm MB4-G): 34,800 repetitions, equating to 191,057 thousand ESALs
- 585RF (45-mm MAC15-G): 3,000 repetitions, equating to 16,470 thousand ESALs

Findings and observations based on the data collected during this HVS study include:

- An aggressive loading regime was followed to induce failure.
- The average maximum rut depths, average maximum deformations and the number of load repetitions to an average maximum rut depth of 12.5 mm (0.5 in) across each entire test section for each test were:
  - 580RF: 18.8 mm (0.8 in), 7.1 mm (0.3 in), and 914 repetitions
  - 581RF: 22.7 mm (0.9 in), 10.3 mm (0.4 in), and 2,324 repetitions
  - 582RF: 15.6 mm (0.6 in), 8.1 mm (0.3 in), and 8,266 repetitions

- 583RF: 31.3 mm (1.3 in), 9.7 mm (0.4 in), and 3,043 repetitions
- 584RF: 23.3 mm (0.9 in), 11.9 mm (0.5 in), and 1,522 repetitions
- 585RF: 23.5 mm (0.9 in), 7.7 mm (0.3 in), and 726 repetitions

- Analysis of surface profiles and test pit observations during a forensic investigation indicate that most of the permanent deformation occurred in the underlying DGAC surfacing layer. The deformation along each section was reasonably uniform, with the exception of Section 584RF (90-mm MB4-G), where more severe rutting and heaving occurred at one end of the test section compared to the other. All of the sections showed some heaving at the sides of the trafficked area, with heights varying between 5 mm (0.2 in) and 16 mm (0.6 in).
- The ranking of rutting performance (keeping in mind that most damage occurred in the underlying DGAC layer), based on the number of repetitions to reach an average maximum rut depth of 12.5 mm, from best to worst is:

1. 582RF: 90-mm AR4000-D (8,266 repetitions)
2. 583RF: 45-mm MB4-G (3,043 repetitions)
3. 581RF: 45-mm RAC-G (2,324 repetitions)
4. 584RF: 90-mm MB4-G (1,522 repetitions)
5. 580RF: 45-mm MB15-G (914 repetitions)
6. 585RF: 45-mm MAC15-G (726 repetitions)

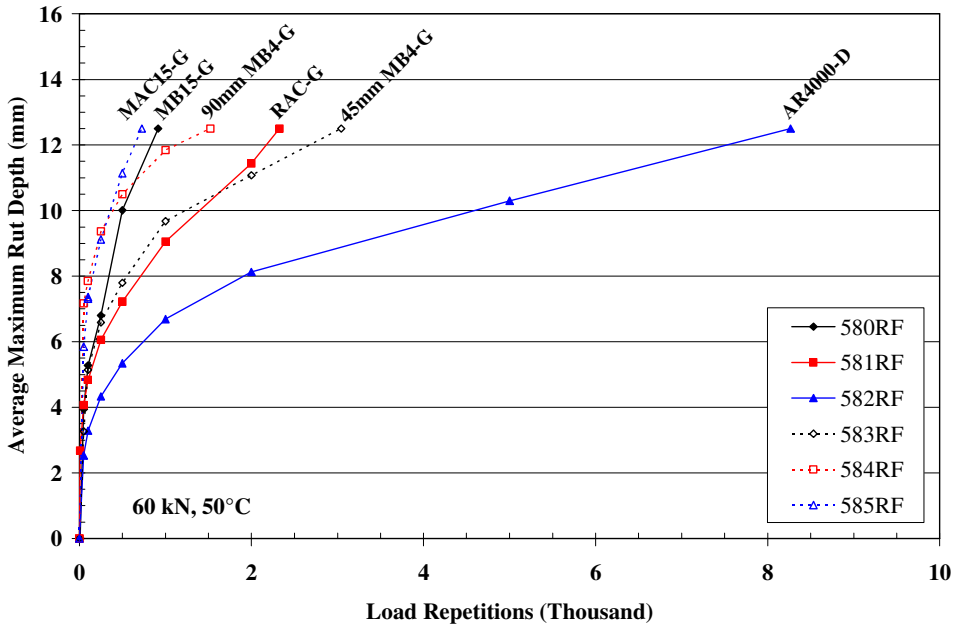

No recommendations as to the use of modified binders in overlay mixes are made at this time. These recommendations will be included in the second-level analysis report, which will be prepared and submitted on completion of all HVS and laboratory testing.

TABLE OF CONTENTS

LIST OF TABLES

LIST OF FIGURES

1. INTRODUCTION

1.1. Objectives

The first-level analysis presented in this report is part of Partnered Pavement Research Center Strategic Plan Element 4.10 (PPRC SPE 4.10) being undertaken for the California Department of Transportation (Caltrans) by the University of California Pavement Research Center (UCPRC). The objective of the study is to evaluate the reflective cracking performance of asphalt binder mixes used in overlays for rehabilitating cracked asphalt concrete pavements in California. The study includes mixes modified with rubber and polymers, and it will develop tests, analysis methods, and design procedures for mitigating reflective cracking in overlays. This work is part of a larger study on modified binder (MB) mixes being carried out under the guidance of the Caltrans Pavement Standards Team (PST) (1), which includes laboratory and accelerated pavement testing using the Heavy Vehicle Simulator (carried out by the UCPRC), and the construction and monitoring of field test sections (carried out by Caltrans).

1.2. Overall Project Organization

This UCPRC project is a comprehensive study, carried out in three phases, involving the following primary elements (2):

- Phase 1
  - The construction of a test pavement and subsequent overlays;
  - Six separate Heavy Vehicle Simulator (HVS) tests to crack the pavement structure;
  - Placing of six different overlays on the cracked pavement;
- Phase 2
  - Six HVS tests to assess the susceptibility of the overlays to high-temperature rutting (Phase 2a);
  - Six HVS tests to determine the low-temperature reflective cracking performance of the overlays (Phase 2b);
  - Laboratory shear and fatigue testing of the various hot-mix asphalts (Phase 2c);
  - Falling Weight Deflectometer (FWD) testing of the test pavement before and after construction and before and after each HVS test;
  - Forensic evaluation of each HVS test section;
- Phase 3
  - Performance modeling and simulation of the various mixes using models calibrated with data from the primary elements listed above.

Phase 1

In this phase, a conventional dense-graded asphalt concrete (DGAC) test pavement was constructed at the Richmond Field Station (RFS) in the summer of 2001. The pavement was divided into six cells, and within each cell a section of the pavement was trafficked with the HVS until the pavement failed by either fatigue (2.5 m/m^2 [0.76 ft/ft^2]) or rutting (12.5 mm [0.5 in]). This period of testing began in the summer of 2001 and was concluded in the spring of 2003. In June 2003 each test cell was overlaid with either conventional DGAC or asphalt concrete with modified binders as follows:

- Full-thickness (90 mm) AR4000-D dense graded asphalt concrete overlay, included as a control for performance comparison purposes (AR-4000 is approximately equivalent to a PG64-16 performance grade binder);
- Full-thickness (90 mm) MB4-G gap-graded overlay;
- Half-thickness (45 mm) rubberized asphalt concrete gap-graded overlay (RAC-G), included as a control for performance comparison purposes;
- Half-thickness (45 mm) MB4-G gap-graded overlay;
- Half-thickness (45 mm) MB4-G gap-graded overlay with minimum 15 percent recycled tire rubber (MB15-G), and
- Half-thickness (45 mm) MAC15-G gap-graded overlay with minimum 15 percent recycled tire rubber.

The conventional overlay was designed using the current (2003) Caltrans overlay design process. The various modified overlays were either full (90 mm [3.5 in]) or half thickness (45 mm [1.7 in]). Mixes were designed by Caltrans. The overlays were constructed in one day.

Phase 2

Phase 2 included high-temperature rutting and low-temperature reflective cracking testing with the HVS as well as laboratory shear and fatigue testing. The rutting tests were started and completed in the fall of 2003. For these tests, the HVS was placed above a section of the underlying pavement that had not been trafficked during Phase 1. A reflective cracking test was next conducted on each overlay from the winter of 2003-2004 to the summer of 2007. For these tests, the HVS was positioned precisely on top of the sections of failed pavement from the Phase 1 HVS tests to investigate the extent and rate of crack propagation through the overlay.

In conjunction with Phase 2 HVS testing, a full suite of laboratory testing, including shear and fatigue testing, was carried out on field-mixed, field-compacted, field-mixed, laboratory-compacted, and laboratory-mixed, laboratory-compacted specimens.

Phase 3

Phase 3 entailed a second-level analysis carried out on completion of HVS and laboratory testing (the focus of this report). This included extensive analysis and characterization of the mix fatigue and mix shear data, backcalculation of the FWD data, performance modeling of each HVS test, and a detailed series of pavement simulations carried out using the combined data.

An overview of the project timeline is shown in Figure 1.1.

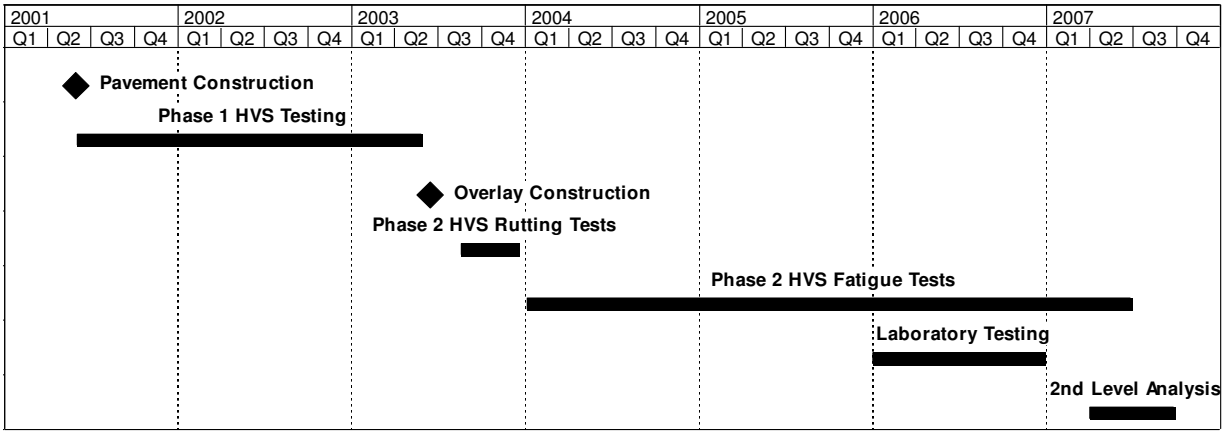

Figure 1.1: Timeline for the Reflective Cracking Study.

Reports

The reports prepared during the reflective cracking study document data from construction, HVS tests, laboratory tests, and subsequent analyses. These include a series of first- and second-level analysis reports and two summary reports. On completion of the study this suite of documents will include:

- One first-level report covering the initial pavement construction, the six initial HVS tests, and the overlay construction (Phase 1);
- One first-level report covering the six Phase 2 rutting tests (but offering no detailed explanations or conclusions on the performance of the pavements);
- Six first-level reports, each of which covers a single Phase 2 reflective cracking test (containing summaries and trends of the measured environmental conditions, pavement responses, and pavement performance but offering no detailed explanations or conclusions on the performance of the pavement);
- One first-level report covering laboratory shear testing;
- One first-level report covering laboratory fatigue testing;
- One report summarizing the HVS test section forensic investigation;
- One report summarizing the backcalculation analysis of deflection tests,

- One second-level analysis report detailing the characterization of shear and fatigue data, pavement modeling analysis, comparisons of the various overlays, and simulations using various scenarios (Phase 3), and
- One four-page summary report capturing the conclusions and one longer, more detailed summary report that covers the findings and conclusions from the research conducted by the UCPRC.

1.3. Structure and Content of this Report

This report presents the results of the Phase 2 rutting tests. It covers the HVS tests on Sections 580RF through 585RF with preliminary analyses relative to observed performance and is organized as follows:

- Chapter 2 contains a description of the test program including experiment layout, loading sequence, instrumentation, and data collection.
- Chapter 3 presents a summary and discussion of the data collected during the test.
- Chapter 4 contains a summary of the results together with conclusions and observations.

1.4. Measurement Units

Metric units have always been used in the design and layout of HVS test tracks, and for all the measurements, data storage, analysis, and reporting at the eight HVS facilities worldwide (as well as all other international accelerated pavement testing facilities). Continued use of the metric system facilitates consistency in analysis, reporting, and data sharing.

In this report, metric and English units are provided in the Executive Summary, Chapters 1 and 2, and the Conclusion. In keeping with convention, only metric units are used in Chapter 3. A conversion table is provided on Page iv at the beginning of this report.

2. TEST DETAILS

2.1. Experiment Layout

Six rutting test sections were constructed as part of the second phase of the study, as follows:

1. Sections 580RF: Half-thickness (45 mm) MB4 gap-graded overlay with minimum 15 percent recycled tire rubber (referred to as "MB15-G" in this report);
2. Sections 581RF: Half-thickness (45 mm) rubberized asphalt concrete gap-graded (RAC-G) overlay;
3. Sections 582RF: Full-thickness (90 mm) AR4000 dense-graded asphalt concrete overlay (designed using CTM356 and referred to as "AR4000-D" in this report);
4. Sections 583RF: Half-thickness (45 mm) MB4 gap-graded overlay (referred to as "45 mm MB4-G" in this report);
5. Sections 584RF: Full-thickness (90 mm) MB4 gap-graded overlay (referred to as "90 mm MB4-G" in this report), and
6. Sections 585RF: Half-thickness (45 mm) MAC15TR gap-graded overlay with minimum 15 percent recycled tire rubber (referred to as "MAC15-G" in this report).

These sections and the corresponding Phase 2 reflective cracking test sections (Sections 586RF through 591RF), tested after completion of the rutting study, are shown in Figure 2.1. The reflective cracking study is discussed in separate first-level analysis reports (3-8).

2.2. Test Section Layout

The general test section layout for each of the rutting sections is shown in Figure 2.2. Station numbers refer to fixed points on the test section and are used for measurements and as a reference for discussing performance.

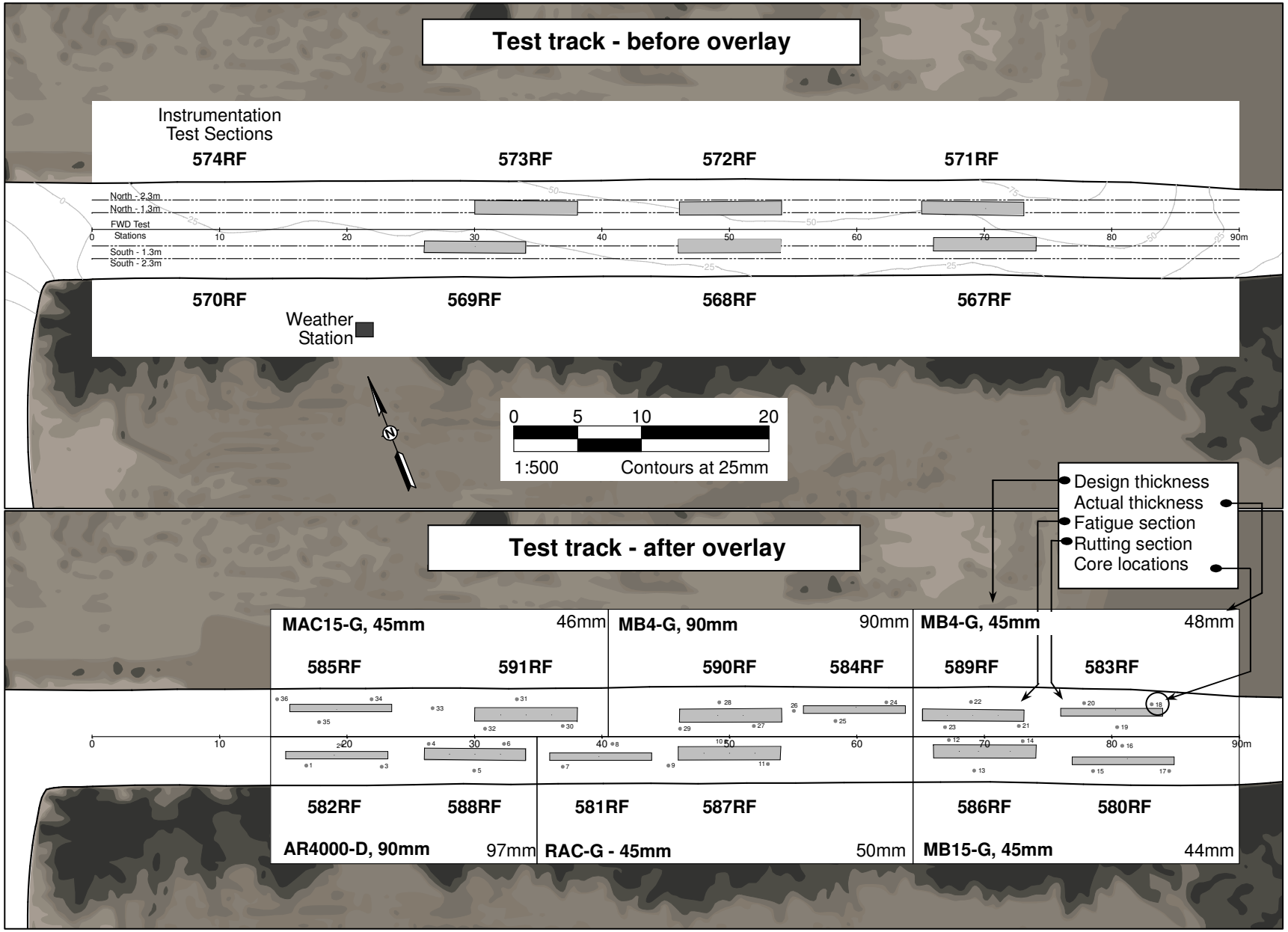

Figure 2.1: Layout of Reflective Cracking Study project.

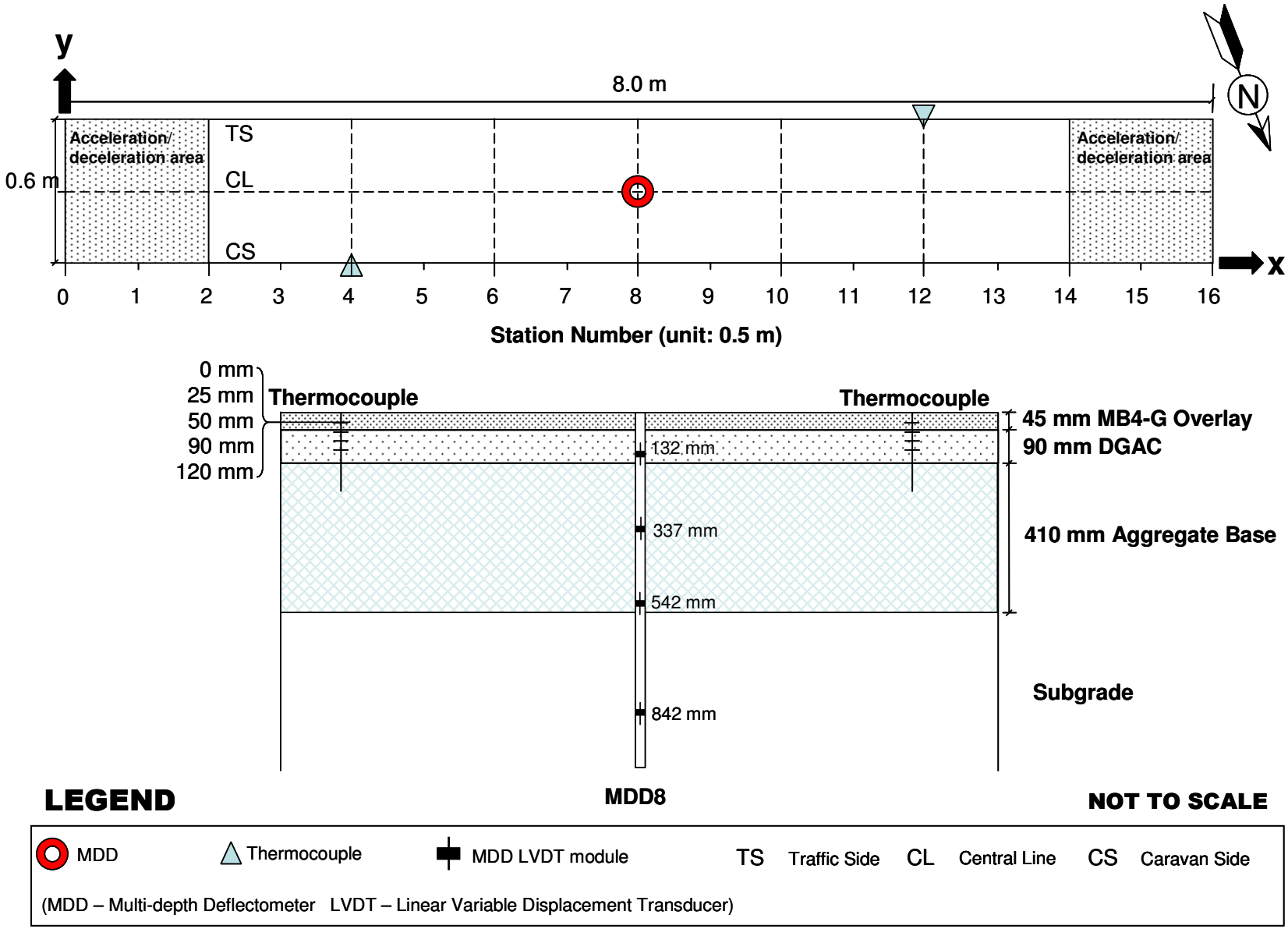

Figure 2.2: Rutting section layout and location of instruments.

2.2.1 Pavement Instrumentation and Monitoring Methods

Measurements were taken with the instruments listed below. Their typical positions are shown in Figure 2.2. Detailed descriptions of the instrumentation and measuring equipment are included in Reference 9. Intervals between measurements, in terms of load repetitions, were selected to enable adequate characterization of the pavement as damage developed.

- Laser Profilometer at each station, measuring surface profile;
- Multi-depth Deflectometer (MDD) at Station 8CL (Station 8 on the centerline of the section), measuring elastic deflection and permanent deformation at different depths in the pavement, and
- Thermocouples, measuring pavement temperature (at Stations 4 and 12) and ambient temperature at one-hour intervals during HVS operation.

Air temperatures were measured at a weather station next to the test section and recorded at the same intervals as the thermocouples.

2.3. Underlying Pavement Design

The pavement for the first phase of HVS trafficking was designed according to the Caltrans Highway Design Manual Chapter 600 using the computer program *NEWCON90.* Design thickness was based on a tested subgrade R-value of 5 and a Traffic Index of 7 (~121,000 ESALs) (10). The pavement design for the test road and the preliminary as-built pavement structures for Sections 580RF through 585RF (determined from cores removed from the edge of the section) are illustrated in Figure 2.3.

The existing subgrade was ripped and reworked to a depth of 200 mm (8 in) so that the optimum moisture content and the maximum wet density met the specification per Caltrans Test Method CTM 216. The average maximum wet density of the subgrade was 2,180 kg/m^3 (136 pcf). The average relative compaction of the subgrade was 97 percent (10).

The aggregate base was constructed to meet the Caltrans compaction requirements for aggregate base Class 2 using CTM 231 nuclear density testing. The maximum wet density of the base determined according to CTM 216 was 2,200 kg/m^3 (137 pcf). The average relative compaction was 98 percent.

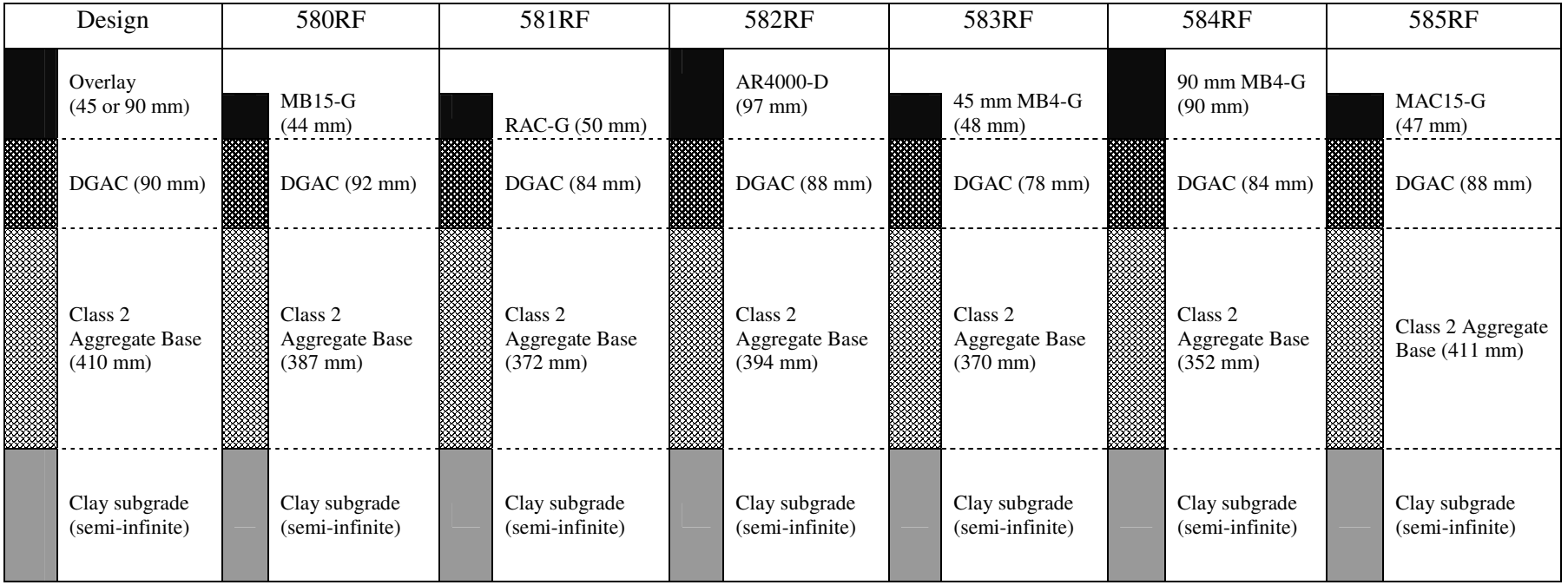

Figure 2.3: Pavement design for the Reflective Cracking Study (design and actual).

The DGAC layer consisted of a dense-graded asphalt concrete (DGAC) with AR-4000 binder and aggregate gradation limits following Caltrans 19-mm (0.75 in) maximum size coarse gradation (10). The target asphalt content was 5.0 percent by mass of aggregate, while actual contents varied between 4.34 and 5.69 percent. Nuclear density measurements and extracted cores were used to determine a preliminary as-built mean air-void content of 9.1 percent with a standard deviation of 1.8 percent. The air-void content after traffic compaction and additional air-void contents from cores taken outside the trafficked area will be determined on completion of trafficking of all sections and will be reported in the second-level analysis report.

The underlying DGAC layer was constructed in September 2001 and was exposed to the elements and some vehicular traffic until the overlays were placed in June 2003.

2.4. Rutting Section Design

The HVS rutting sections were located on the overlays adjacent to the reflective cracking sections, which were precisely located on top of the previously trafficked sections on the underlying DGAC layer. The overlay thickness for the experiment was determined according to Caltrans Test Method CTM 356 using Falling Weight Deflectometer data from the Phase 1 experiment. The actual layer thicknesses of the sections were measured from cores extracted from the edge of the test sections, test pit observations, and from Dynamic Cone Penetrometer (DCP) tests. The measured thicknesses for the sections are summarized in Table 2.1.

Table 2.1: Average Pavement Thicknesses

Section	Layer	Thickness (mm) [in]			Standard Deviation (mm) [in]
		Average	Minimum	Maximum	
580RF MB15-G	Overlay	44 [1.8]	35 [1.4]	54 [2.2]	9.7 [0.4]
	DGAC	92 [3.7]	86 [3.4]	101 [4.0]	7.7 [0.3]
	Base	387 [15.5]	357 [14.3]	428 [17.1]	26.0 [1.0]
581RF RAC-G	Overlay	50 [2.0]	41 [1.6]	56 [2.2]	6.1 [0.2]
	DGAC	84 [3.4]	77 [3.1]	90 [3.6]	4.4 [0.2]
	Base	372 [14.9]	339 [13.6]	393 [15.7]	17.0 [0.7]
582RF AR4000-D	Overlay	97 [3.9]	85 [3.4]	105 [4.2]	8.6 [0.3]
	DGAC	88 [3.5]	85 [3.4]	103 [4.1]	8.0 [0.3]
	Base	394 [15.8]	385 [15.4]	400 [16.0]	6.0 [0.2]
583RF 45 mm MB4-G	Overlay	48 [1.9]	42 [1.7]	54 [2.2]	4.5 [0.2]
	DGAC	78 [3.1]	64 [2.6]	94 [3.8]	12.2 [0.5]
	Base	370 [14.8]	343 [13.7]	396 [15.8]	16.0 [0.6]
584RF 90 mm MB4G	Overlay	90 [3.6]	82 [3.3]	101 [4.0]	7.8 [0.3]
	DGAC	84 [3.4]	73 [2.9]	93 [3.7]	7.5 [0.3]
	Base	352 [14.1]	310 [12.4]	347 [13.9]	11.0 [0.4]
585RF MAC15-G	Overlay	97 [3.9]	85 [3.4]	105 [4.2]	8.6 [0.3]
	DGAC	88 [3.5]	85 [3.4]	103 [4.1]	8.0 [0.3]
	Base	411 [16.4]	404 [16.2]	422 [16.9]	4.0 [0.2]

Laboratory testing was carried out by Caltrans and UCPRC on samples collected during construction to determine actual binder properties, binder content, aggregate gradation, and air-void content. The binders met the Caltrans binder specifications, based on testing performed by Caltrans. The average ignition-extracted binder contents of the various layers, corrected for aggregate ignition and compared to the design binder content are listed in Table 2.2. Actual binder contents were in all instances higher than the design binder content. It is not clear whether this is a function of the test or contractor error.

Table 2.2: Design vs. Actual Binder Contents

Section	Overlay	Binder Content (%)	
		Design	Actual
580RF	MB15-G	7.1	7.52
581RF	RAC-G	8.0	8.49
582RF	AR4000-D	5.0	6.13
583RF	45 mm MB4-G	7.2	7.77
584RF	90 mm MB4-G	7.2	7.77
585RF	MAC15-G	7.4	7.55

The aggregate gradations for the AR4000-D and modified binders generally met Caltrans specifications for 19.0 mm (3/4 inch) maximum size course and gap gradations respectively, with specifics for each section detailed below. Gradations are illustrated in Figures 2.4 (modified binders) and 2.5 (AR4000-D).

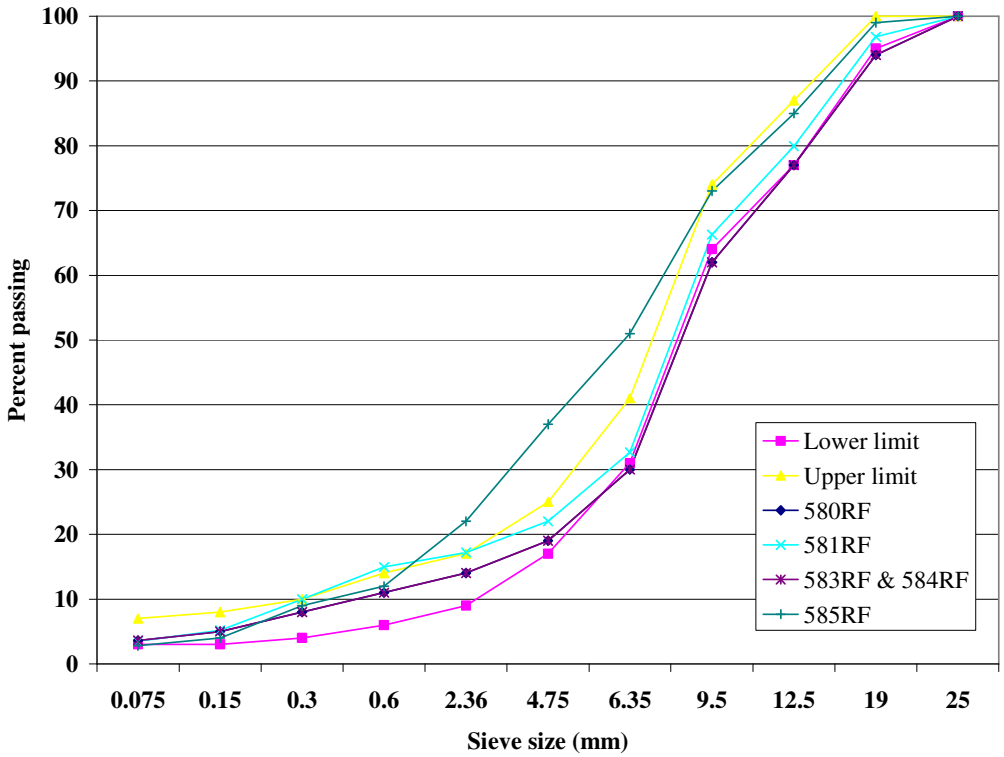

Figure 2.4: Gradation for modified binder overlays.

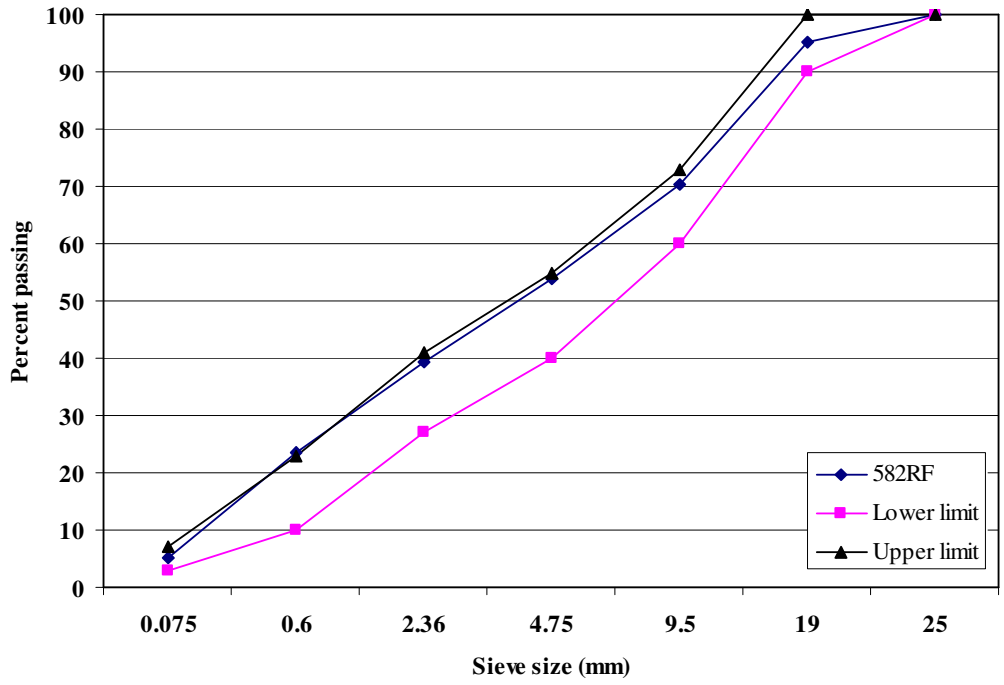

Figure 2.5: Gradation for AR4000-D overlay.

- 580RF: Material passing the 6.35 mm (1/4 in), 9.5 mm (3/8 mm), 12.5 mm (1/2 in), and 19.0 mm (3/4 in) sieves was on the lower envelope limit (Figure 2.4).
- 581RF: Material passing the 0.3 mm (#50), 0.6 mm (#30), and 2.36 mm (#8) sieves was on the upper envelope limit (Figure 2.4).
- 582RF: Material passing the 0.6 mm (#30), 2.36 mm (#8), and 4.75 mm (#4) sieves was on the upper envelope limit (Figure 2.5).
- 583RF: Material passing the 6.35 mm (1/4 in) and 9.5 mm (3/8 in) sieves was on the lower envelope limit (Figure 2.4).
- 584RF: Material passing the 6.35 mm (1/4 in) and 9.5 mm (3/8 in) sieves was on the lower envelope limit (Figure 2.4).
- 585RF: Material passing the 0.6 mm (#30), 9.5 mm (3/8 in), 12.5 mm (1/2 in), and 19.0 mm (3/4 in) sieves was on the upper envelope limit, while material passing the 2.36 mm (#8), 4.75 mm (#4), and 6.35 mm (1/4 in) sieves was outside the upper limit (Figure 2.4).

The overlays were placed on the same day, within a few hours of each other. A tack coat was applied prior to placement. The 90 mm layers were placed in two lifts of 45 mm and a tack coat was applied between lifts. The preliminary as-built air-void contents for each section, based on cores taken outside of the HVS sections prior to HVS testing, are listed in Table 2.3.

Table 2.3: Air-Void Contents

Section	Overlay	Air-Void Content (%)	
		Average for Section	Standard Deviation
580RF	MB15-G	5.1	1.7
581RF	RAC-G	8.8	1.3
582RF	AR4000-D	7.1	1.5
583RF	45 mm MB4-G	6.5	0.6
584RF	90 mm MB4-G	6.5	0.6
585RF	MAC15-G	4.9	1.0

2.5. Summary of Testing on Rutting Section

2.5.1 Test Section Failure Criteria

An average maximum rut of 12.5 mm (0.5 in) over the full monitored section (Station 3 to Station 13) was set as the failure criteria for the experiment.

2.5.2 Environmental Conditions

The pavement surface temperature was maintained at 50°C±4°C (122°F±7°F) to assess rutting potential under typical pavement conditions. Infrared heaters inside a temperature control chamber (11) were used to maintain the pavement temperatures. The pavement surface received no direct rainfall as it was protected by the temperature control chamber. The sections were tested predominantly during the wet season (September to December) and hence water infiltration into the pavement from the side drains and through the raised groundwater table was possible.

2.5.3 Test Duration

HVS trafficking on each section was initiated and completed as shown in Table 2.4 and Figure 2.6. It should be noted that on certain tests, trafficking was continued beyond failure to allow the collection of additional performance data.

Table 2.4: Test Duration for the HVS Rutting Tests

Section	Overlay	Start Date	Finish Date	Repetitions
580RF	MB15-G	09/29/03	10/01/03	2,000
581RF	RAC-G	09/15/03	09/19/03	7,600
582RF	AR4000-D	09/04/03	09/09/03	18,564
583RF	45 mm MB4-G	12/08/03	12/16/03	15,000
584RF	90 mm MB4-G	11/13/03	11/26/03	34,800
585RF	MAC15-G	10/10/03	10/20/03	3,000

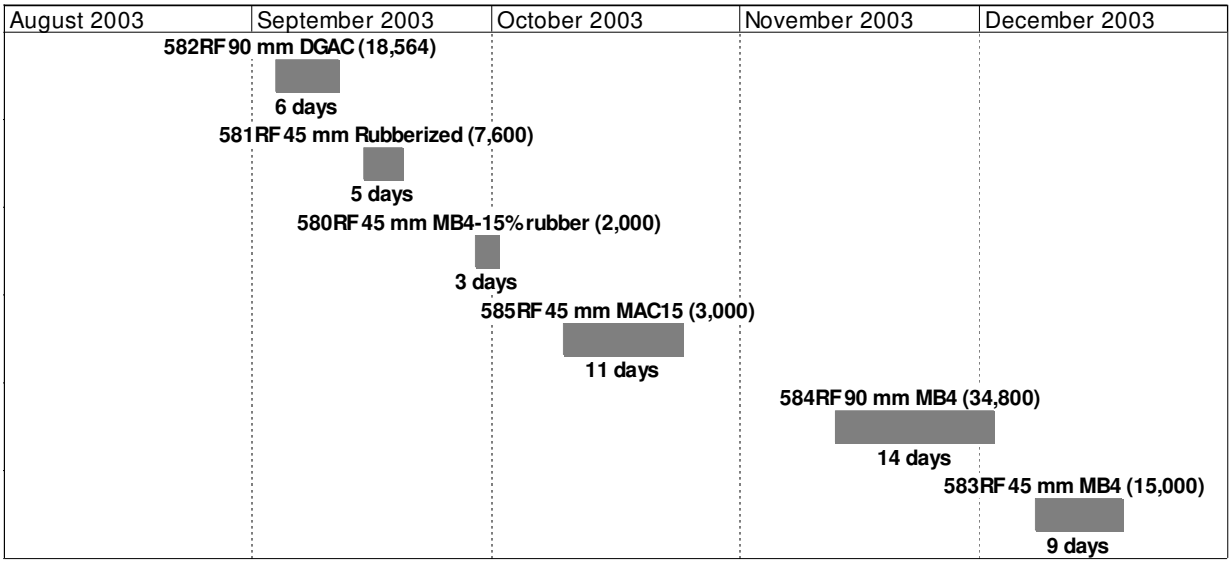

Figure 2.6: Trafficking schedule for the HVS rutting tests.

2.5.4 Loading Program

The HVS loading program for each section is summarized in Table 2.5. All trafficking was carried out with a dual-wheel configuration, using radial truck tires (Goodyear G159 - 11R22.5- steel belt radial) inflated to a pressure of 720 kPa (104 psi), in a channelized, unidirectional loading mode. The loading program followed differs from the original test plan due to an incorrect hydraulic control system setup on loads less than 65 kN (14,600 lb) in the Phase 1 experiment. The loading pattern from the Phase 1 experiment was thus retained to facilitate comparisons of performance between all tests in the Reflective Cracking Study.

Table 2.5: Summary of HVS Loading Program

Section	Overlay	Start Repetition	Wheel Load (kN) - [lb]		ESALs	Traffic Index
			Planned	Actual*		
580RF	MB15-G	Full test	40 [9,000]	60 [13,500]	11,000	N/A
581RF	RAC-G				42,000	N/A
582RF	AR4000-D				102,000	N/A
583RF	45 mm MB4-G				83,000	N/A
584RF	90 mm MB4-G				191,000	N/A
585RF	MAC15-G				17,000	N/A

* The loading program differs from the original test plan due to an incorrect hydraulic control system setup on loads less than 65 kN in the Phase 1 experiment. The loading pattern from the Phase 1 experiment was thus retained to facilitate comparisons of performance between all tests in the Reflective Cracking Study.

3. DATA SUMMARY

3.1. Introduction

This chapter provides a summary of the data collected from Sections 580RF through 585RF and a brief discussion of the first-level analysis. Data collected included rainfall, air temperatures inside and outside the temperature control chamber, pavement temperatures, in-depth elastic deflections, and surface and in-depth permanent deformation.

Pavement temperatures were controlled using the temperature control chamber. Both air (inside and outside the temperature box) and pavement temperatures were monitored and recorded hourly during the entire loading period. In assessing rutting performance, the temperature at the bottom of the asphalt concrete and the temperature gradient are the two important controlling temperature parameters used to evaluate the stiffness of the asphalt concrete and to compute the plastic strain as accurately as possible.

Elastic (recoverable) deflections provide an indication of the overall stiffness of the pavement structure and, therefore, a measure of the load-carrying capacity. As the stiffness of a pavement structure deteriorates, its ability to resist the deformation/deflection caused by a given load and tire pressure decreases. During HVS testing, elastic deflections are normally measured with two instruments. The Road Surface Deflectometer (RSD) measures surface deflections and Multi-depth Deflectometers (MDD) measures in-depth deflections. However, due to the nature of the deformation and resulting uneven surface on these rutting tests, RSD measurements were not taken. Since MDD modules could not be installed at the surface due to the limited thickness of the overlay, no surface deflections during testing were recorded. However, Falling Weight Deflectometer (FWD) measurements were taken across the section after the construction of the overlays (10) and prior to starting the HVS reflective cracking testing. FWD results will be discussed in the second level analysis report.

Permanent deformation at the pavement surface (rutting) was monitored with the Laser Profilometer and at various depths within the pavement with a single set of MDD modules. The reference point for the MDD modules was three meters below the pavement surface. The following rut parameters were determined from these measurements (9), as illustrated in Figure 3.1:

- Average maximum rut depth (average of the maximum rut depth at each measuring station)
- Average deformation
- Location and magnitude of the maximum rut depth, and
- Rate of rut development.

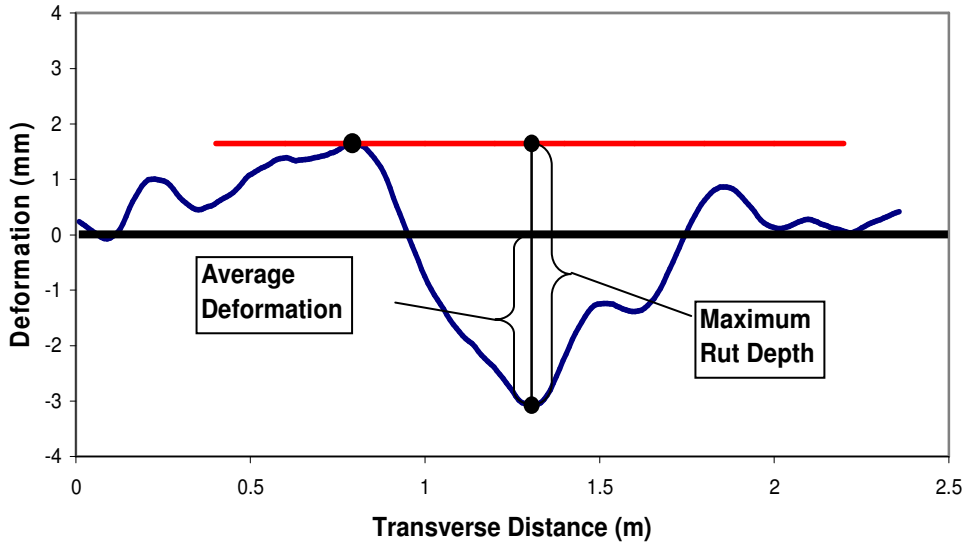

Figure 3.1: Illustration of maximum rut depth and average deformation of a leveled profile.

The Laser Profilometer provides sufficient information to evaluate the evolution of permanent surface deformation of the entire test section at various loading stages. The rut depth figures in this report show the average values over the entire section (Stations 3 through 13) as well as values for half sections between Stations 3 and 8 and Stations 9 and 13. These two additional data series were plotted to illustrate any differences along the length of the section.

The accumulation of vertical deformation at various depths in the pavement was measured with the MDD Linear Variable Displacement Transducer (LVDT) modules during the course of the HVS test. Permanent deformation measured by each LVDT is the total permanent deformation of the pavement between the anchoring depth (3.0 m) and the depth of the module. Accordingly, LVDT modules in the upper part of the pavement typically measure larger permanent deformation than those in the lower part. The difference in measured permanent deformation between two LVDT modules represents the permanent deformation accumulated in the layers between those two modules. This is known as differential permanent deformation. The permanent in-depth MDD data is normally presented along with the surface deformation measured with the Laser Profilometer as this allows determination of the rutting in the asphalt concrete (AC) layer(s). However, in this report, the presentation of the surface data has been omitted from the figures since the majority of the rutting occurred in the asphalt concrete layers and the inclusion of this data would distort the scale of the figures.

The data from each test is presented separately, with the presentation of each test following the same format. Data plots are presented on the same scale to facilitate comparisons of performance. Interpretation

of the data in terms of pavement performance will be discussed in a separate second-level analysis report. Details of the forensic investigation are presented in Reference 12.

3.2. Rainfall

Figure 3. shows the monthly rainfall data from September 2003 to December 2003 as adapted from the weather station at the Richmond Field Station HVS site. The first four tests (582RF, 581RF, 580RF, and 585RF) were completed in dry conditions. During tests on Sections 583RF and 584RF, 144 mm (5.75 in) of rain was recorded.

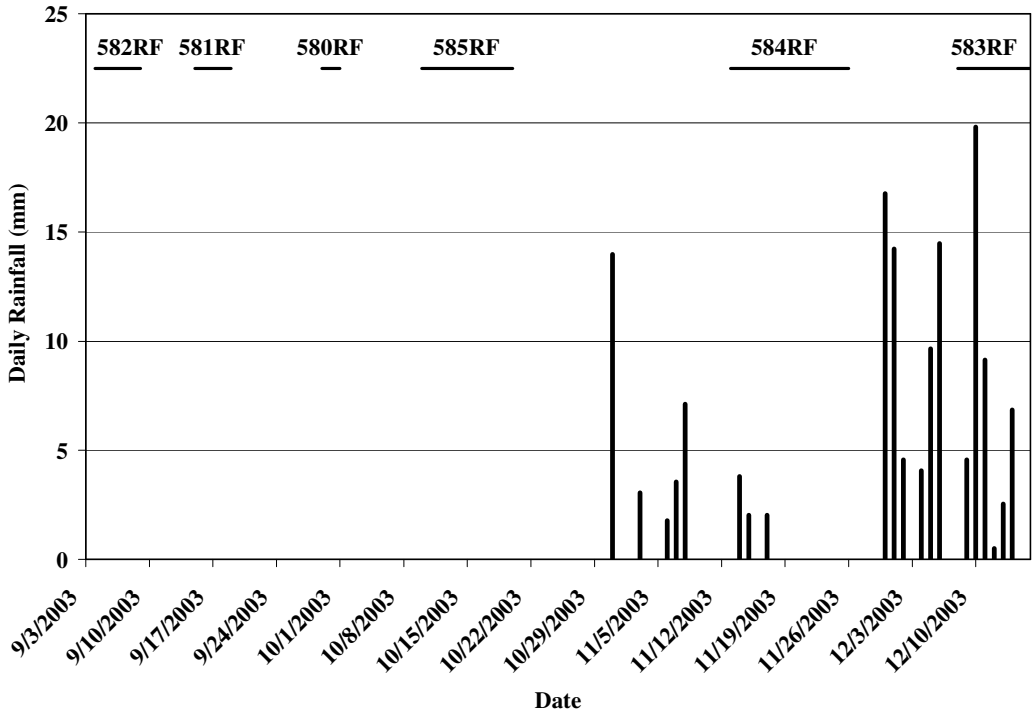

Figure 3.2: Measured rainfall at the Richmond Field Station during the HVS testing.

3.3. Section 580RF: 45-mm MB4-G

3.3.1 Test Summary

Loading commenced on September 29, 2003, and ended on October 1, 2003. During this period 2,000 load repetitions were applied and seven datasets were collected.

3.3.2 Air Temperatures in the Temperature Control Unit

During the test, air temperatures inside the temperature control chamber ranged from 50°C to 58°C with an average of 52°C and standard deviation of 1.4°C. Air temperatures were adjusted to maintain a pavement temperature of 50°C±4°C, which is expected to promote rutting damage. The daily average air

temperatures recorded in the temperature control unit, calculated from the hourly temperatures recorded during HVS operation, are shown in Figure 3.3. Vertical errors bars on each point on the graph show daily temperature range.

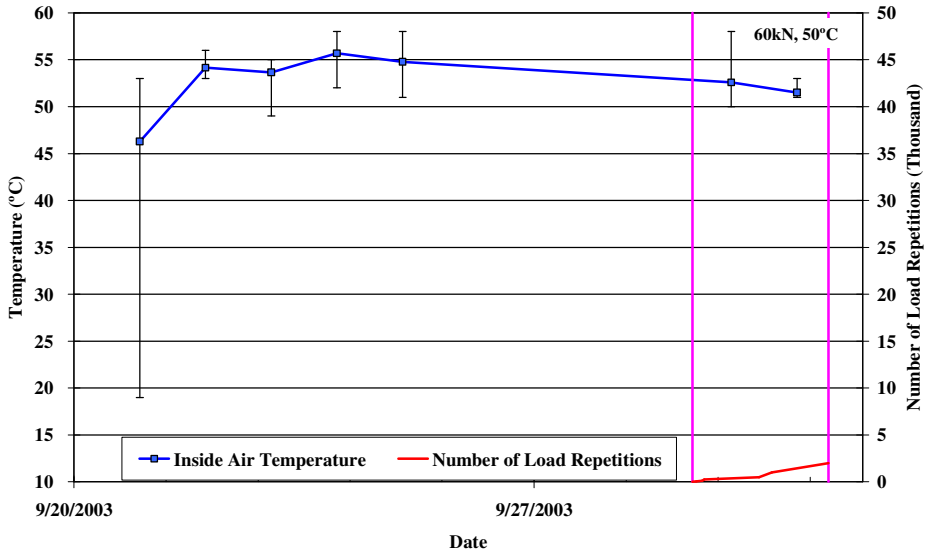

Figure 3.3: 580RF: Daily average air temperatures inside the temperature control chamber.

3.3.3 Outside Air Temperatures

Outside air temperatures ranged from 13°C to 19°C with an average of 14.5°C and are summarized in Figure 3.4. Vertical error bars on each point on the graph show daily temperature range.

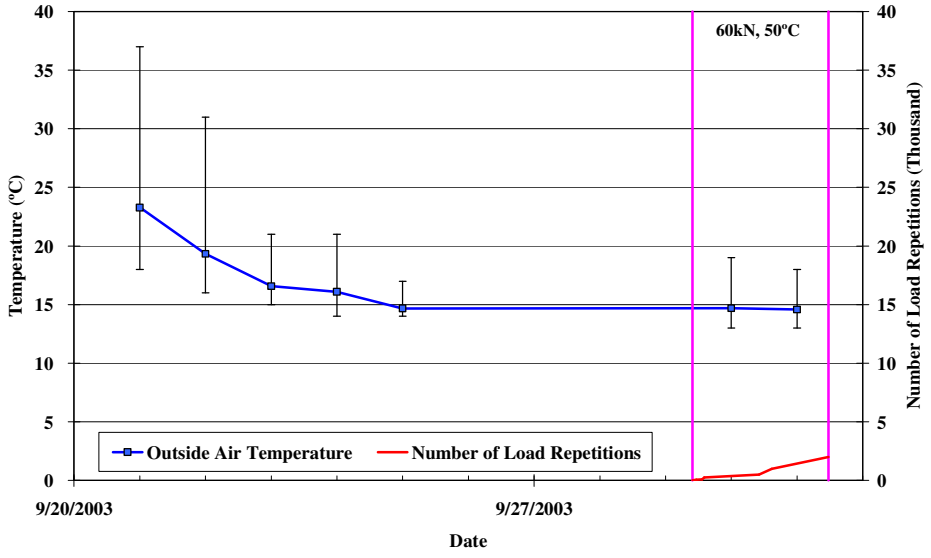

Figure 3.4: 580RF: Daily average air temperatures outside the temperature control chamber.

3.3.4 Temperatures in the Asphalt Concrete Layer

Daily averages of the surface and in-depth temperatures of the asphalt concrete layer are listed in Table 3.1 and shown in Figure 3.5. Pavement temperatures decreased slightly with increasing depth in the pavement. This is expected as there is a significant thermal gradient between the pavement surface and the natural soil.

Table 3.1: 580RF: Temperature Summary for Air and Pavement.

Temperature	Average (°C)	Std Dev (°C)
Outside air	14.5	1.3
Inside air	52.1	1.4
Pavement surface	51.7	3.7
- 25 mm below surface	50.3	3.6
- 50 mm below surface	49.1	3.3
- 90 mm below surface	48.3	3.2
- 120 mm below surface	47.5	3.1

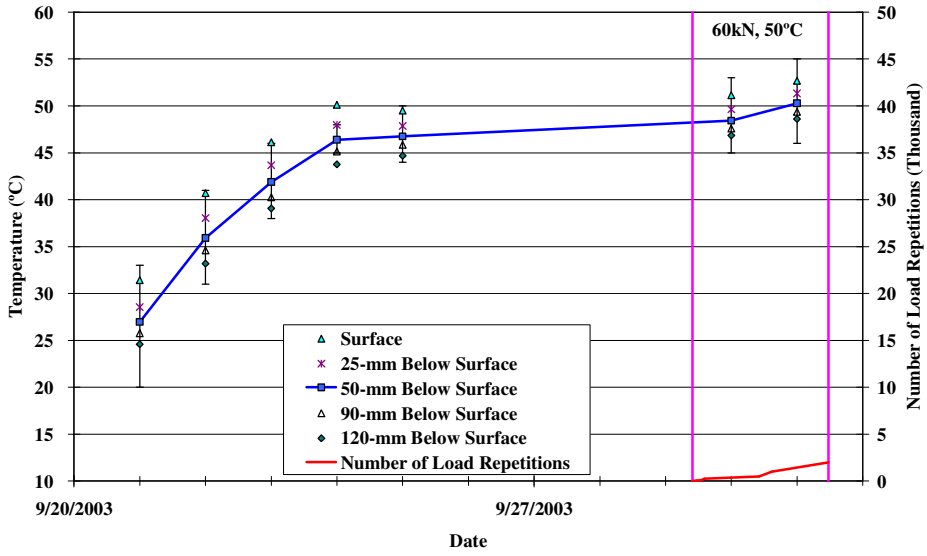

Figure 3.5: 580RF: Daily average temperatures at pavement surface and various depths.

3.3.5 In-Depth Elastic Deflection from MDD

Measurements of in-depth elastic deflection from the MDDs were made with a test load of 60 kN at various times during trafficking. Table 3.2 and Figure 3.6 summarize the in-depth elastic deflections measured at various depths with MDD8.

Table 3.2: 580RF: Summary of 60 kN In-Depth Elastic Deflections.

Depth (mm)	Layer	Elastic Deflection at 60 kN (microns)		
		Before Trafficking	After Trafficking	Ratio of Final/Initial
122	Bottom of underlying DGAC	659	764	1.16
327	Middle of aggregate base	309	338	1.09
542	Bottom of aggregate base	Not recorded	Not recorded	Not recorded
847	300 mm below top of subgrade	195	230	1.18

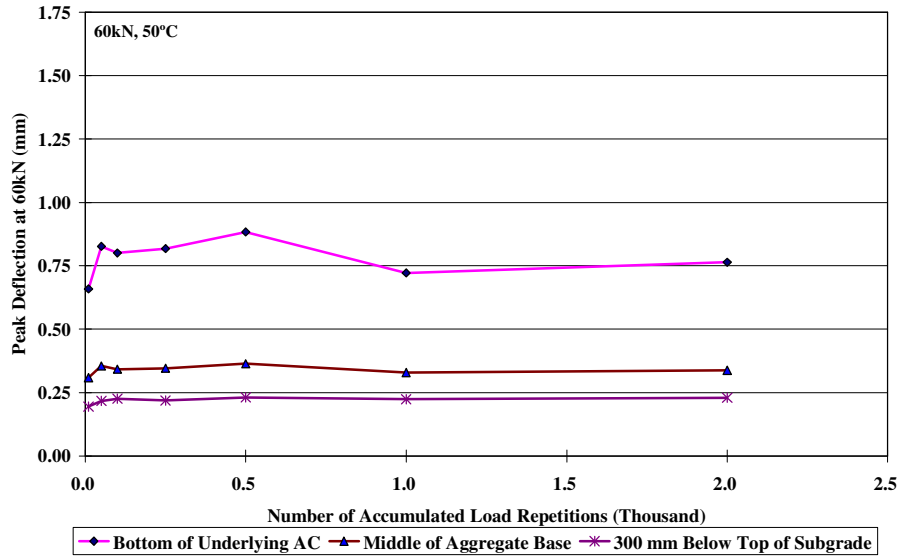

Figure 3.6: 580RF: Elastic deflections at MDD8 with 60 kN test load.

The following observations were made from the data collected:

- The elastic deflections increased slightly at the beginning of the experiment, which is typical.
- The effect of trafficking load on elastic deformation decreases with increasing depth, as expected. Most of the damage observed appeared to occur in the upper portion of the pavement. This was verified from observations and measurements of a test pit profile (12).
- Ratios of final-to-initial MDD deflections show that deflections had increased slightly (between 9 and 18 percent) at all depths in the pavement structure at the end of trafficking. This loss of stiffness indicates damage in the asphalt concrete layers, which increases shear stresses in the underlying layers.

3.3.6 Permanent Surface Deformation (Rutting)

Figure 3.7 shows the average transverse cross section measured with the Laser Profilometer at various stages of the test. This plot clearly shows the increase in rutting and deformation over the duration of the test.

During HVS testing, rutting usually occurs at a high rate initially and then typically diminishes as trafficking progresses until reaching a steady state. This initial phase is referred to as the "embedment" phase. Figures 3.8 and 3.9 show the development of permanent deformation (average maximum rut and average deformation, respectively) with load repetitions as determined by the Laser Profilometer for the test section, with an embedment phase only apparent at the beginning of the experiment. Error bars on the average reading indicate variation along the length of the section. Figure 3.10 shows a contour plot of the pavement surface at the end of the test (2,000 repetitions). After completion of trafficking, the average

maximum rut depth and the average deformation were 18.8 mm and 7.1 mm, respectively. The maximum rut depth measured on the section was 22.3 mm. Rut development was rapid with the failure criteria of an average of 12.5 mm total rut depth reached after 914 load repetitions.

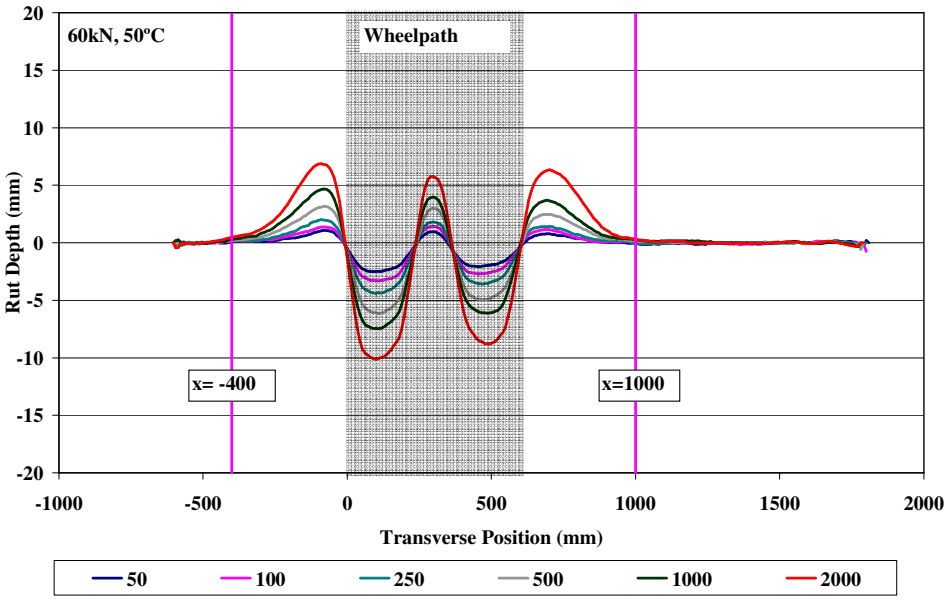

Figure 3.7: 580RF: Profilometer cross section at various load repetitions.

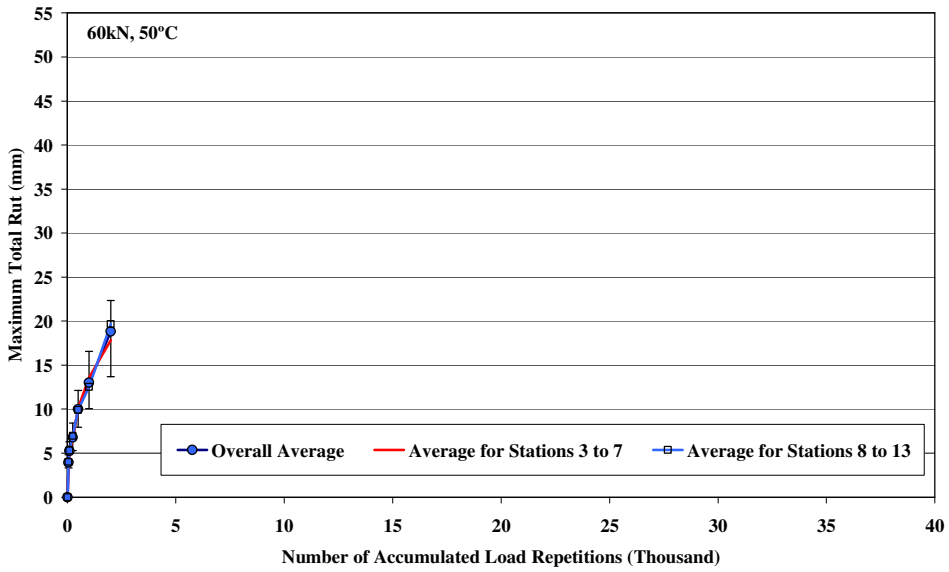

Figure 3.8: 580RF: Average maximum rut.

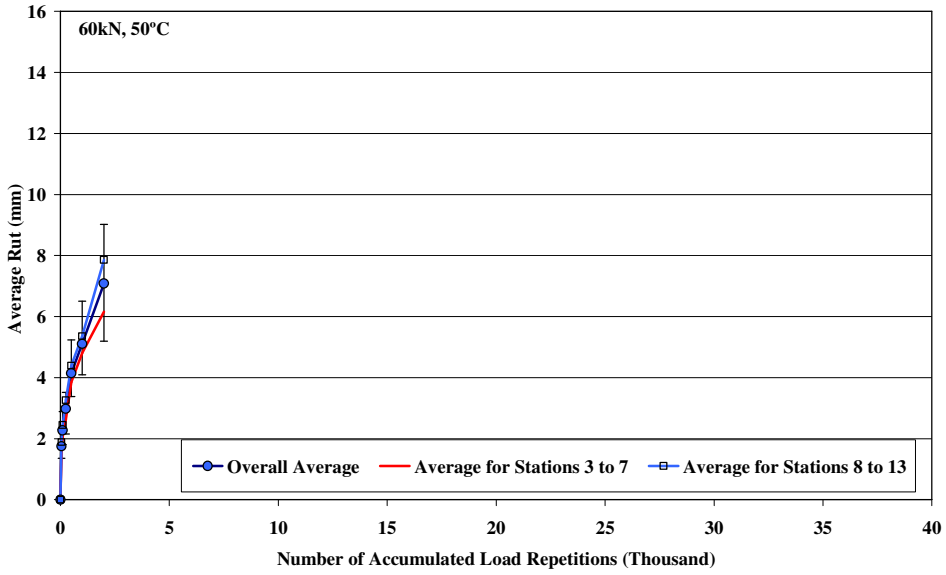

Figure 3.9: 580RF: Average deformation.

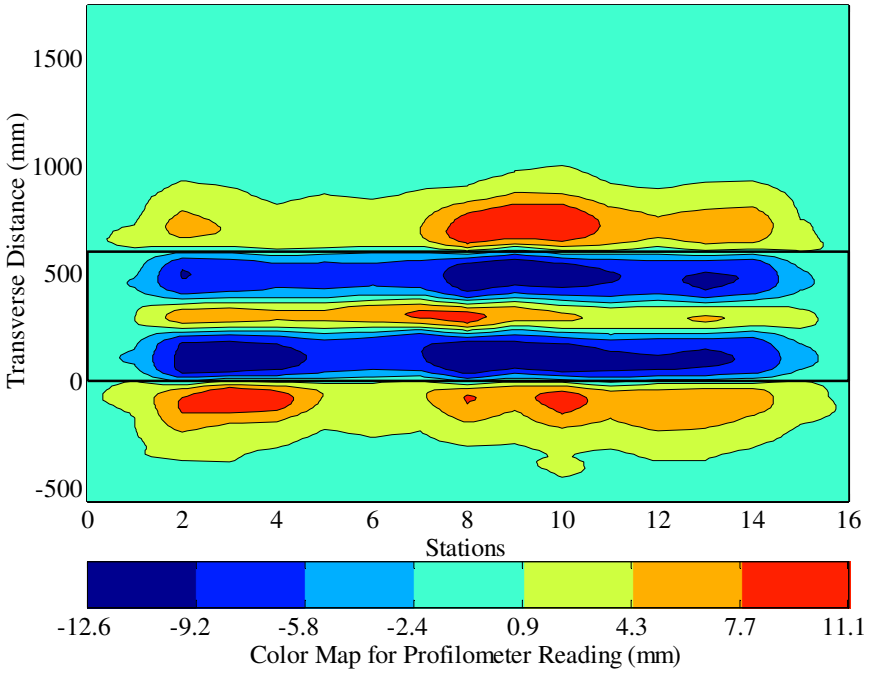

Figure 3.10: 580RF: Contour plot of permanent surface deformation after 2,000 repetitions.

3.3.7 Permanent In-Depth Deformation

Permanent in-depth deformation was measured with MDD modules were installed at Station 8, at the following depths. A module was not installed on the surface of the overlay due to thickness constraints.

- 122 mm: near the bottom of the underlying DGAC layer
- 327 mm: in the middle of the aggregate base layer
- 542 mm: at the bottom of the aggregate base layer (not functioning in this test)
- 722 mm: 300 mm below the top of the subgrade

Table 3.3 and Figures 3.11 and 3.12 provide an indication of the permanent deformation recorded at MDD8. Figure 3.11 shows the permanent deformation at the MDD modules, while Figure 3.12 shows the permanent deformation calculated for the various layers. The data shows that the majority of the permanent deformation occurred in the asphalt concrete layers (88 percent). This was verified after excavation and assessment of a test pit, where it was found that the deformation in the asphalt concrete layers was almost completely attributable to the underlying DGAC layer (12). Approximately 2.0 mm of rutting occurred in the overlay and approximately 20 mm in the underlying DGAC. Slight differences between the data obtained from the MDDs and the test pit profile are attributed to the difference in location of the MDD and the test pit profile, and the resolution of the measurements on the profile (~1.0 mm resolution at best).

Table 3.3: 580RF: Vertical Permanent Deformation in Pavement Layers.

Layer	Nominal Thickness (mm)	Vertical Permanent Deformation (mm)	Percentage Total Deformation (%)
AC layers	135	19.7	88
Upper aggregate base	205	2.4	11
Lower aggregate base	205	0.1	1
Top 300 mm of subgrade	300		
Subgrade to anchor	2,158	<0.1	0
Total (All Layers)	3,000	22.2	100

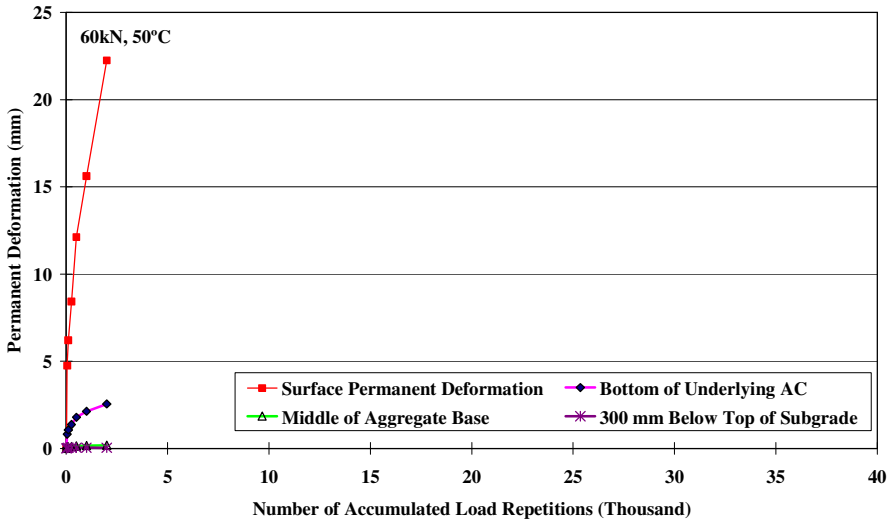

Figure 3.11: 580RF: Permanent in-depth deformation at MDD8.

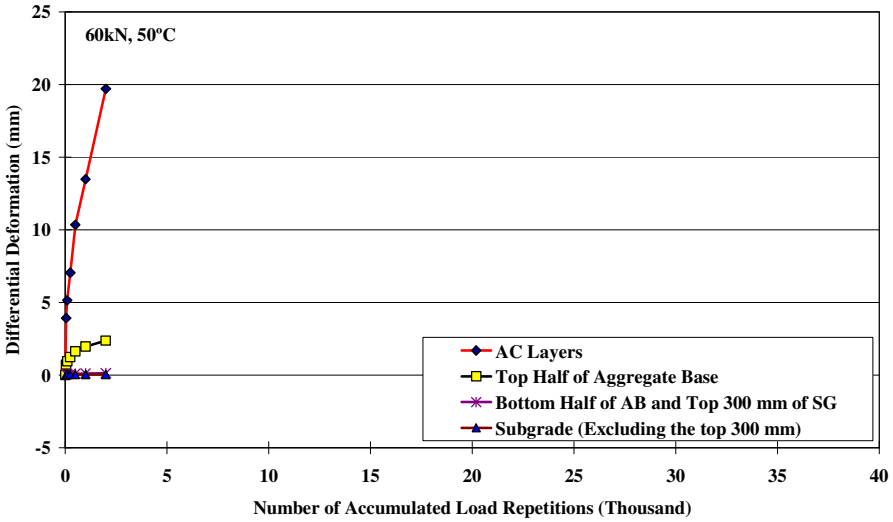

Figure 3.12: 580RF: In-depth differential deformation at MDD8.

3.3.8 Visual Inspection

Apart from rutting, no other distress was recorded on the section. Figure 3.13 shows photographs taken of the surface at the end of the test.

Figure 3.13: 580RF: Section photographs at the end of the test.

3.4. Section 581RF: 45 mm RAC-G

3.4.1 Test Summary

Loading commenced on September 15, 2003 and ended on September 19, 2003. During this period 7,600 load repetitions were applied and nine datasets were collected.

3.4.2 Air Temperatures in the Temperature Control Unit

Air temperatures inside the temperature control chamber ranged from 51°C to 57°C, with an average of 53°C and standard deviation of 3.2°C. Air temperatures were adjusted to maintain a pavement temperature of 50°C±4°C. The daily average air temperatures recorded in the temperature control unit, calculated from the hourly temperatures recorded during HVS operation, are shown in Figure 3.14. Vertical errors bars show daily temperature range.

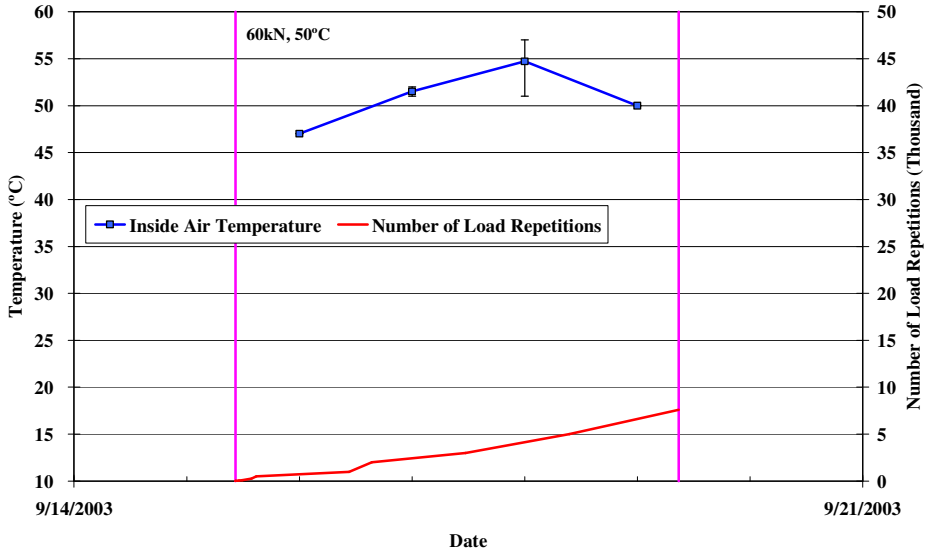

Figure 3.14: 581RF: Daily average air temperatures inside the temperature control chamber.

3.4.3 Outside Air Temperatures

Outside air temperatures ranged from 15°C to 31°C with an average of 22.9°C and are summarized in Figure 3.15. Vertical error bars on each point on the graph show daily temperature range.

3.4.4 Temperatures in the Asphalt Concrete Layer

Daily averages of the surface and in-depth temperatures in the asphalt concrete layer are listed in Table 3.4 and shown in Figure 3.16. Pavement temperatures decreased slightly with increasing depth in the pavement.

Table 3.4: 581RF: Temperature Summary for Air and Pavement.

Temperature	Average (°C)	Std Dev (°C)
Outside air	22.8	5.9
Inside air	53.0	3.2
Pavement surface	50.0	2.6
- 25 mm below surface	49.5	3.1
- 50 mm below surface	48.5	2.8
- 90 mm below surface	47.3	2.4
- 120 mm below surface	46.6	2.3

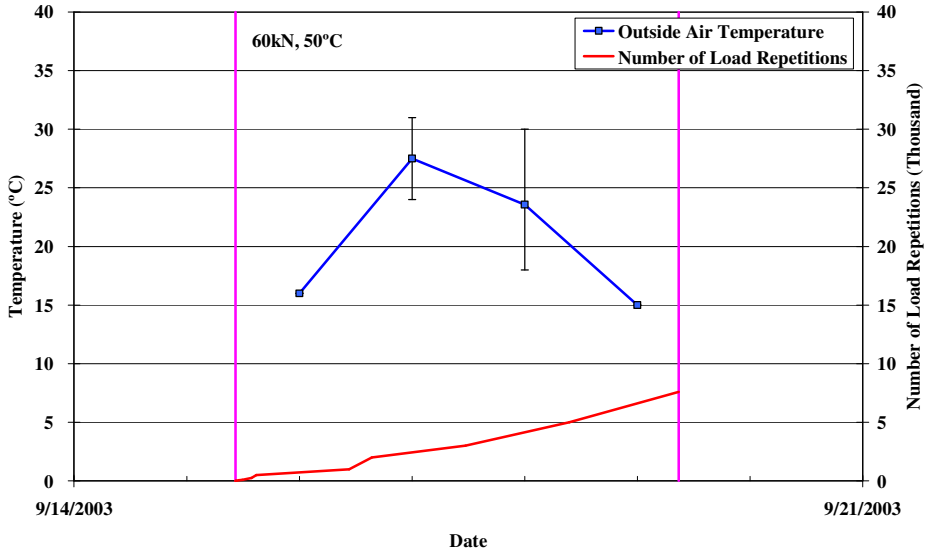

Figure 3.15: 581RF: Daily average air temperatures outside the temperature control chamber.

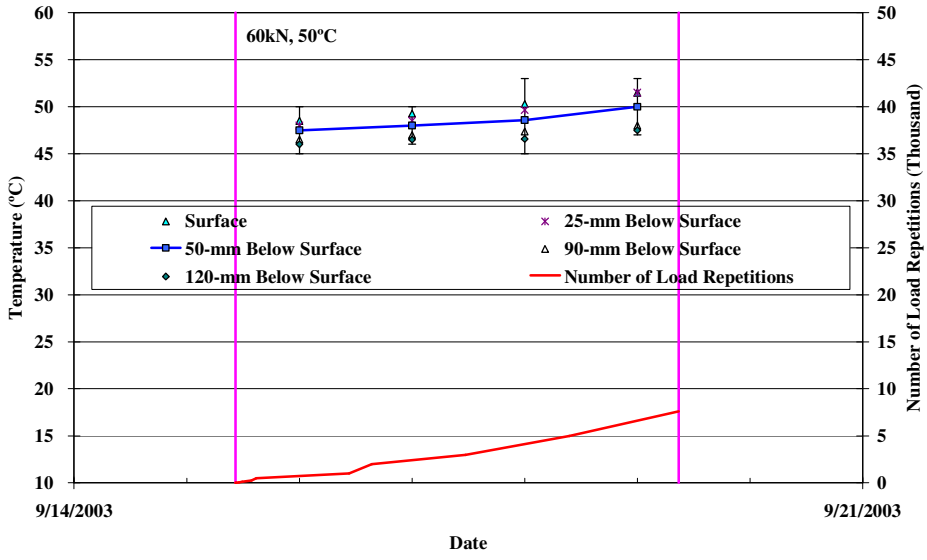

Figure 3.16: 581RF: Daily average temperatures at pavement surface and various depths.

3.4.5 In-Depth Elastic Deflection from MDD

In-depth elastic deflection measurements from the MDD were made with a test load of 60 kN at various times during trafficking. Table 3.5 and Figure 3.17 summarize the in-depth elastic deflections measured at various depths with MDD8.

Table 3.5: 581RF: Summary of 60 kN In-depth Elastic Deflections.

Depth (mm)	Layer	Elastic Deflection at 60 kN (microns)		
		Before Trafficking	After Trafficking	Ratio of Final/Initial
120	Bottom of underlying DGAC	0.945	1.508	1.60
325	Middle of aggregate base	0.857	1.401	1.63
530	Bottom of aggregate base	0.691	1.111	1.61

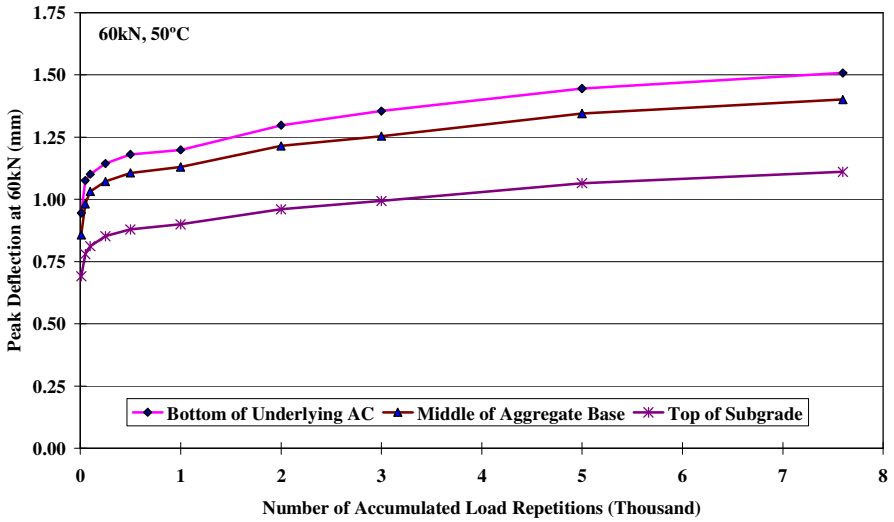

Figure 3.17: 581RF: Elastic deflections at MDD8 with 60 kN test load.

The following observations were made from the data collected:

- The elastic deflections increased slightly at the beginning of the experiment. Deflections continued to increase slowly throughout the test.
- The effect of trafficking load on elastic deformation decreased with increasing depth, as expected. Most of the damage observed appeared to occur in the upper portion of the pavement. This was verified from a test pit profile (12).
- Ratios of final-to-initial MDD deflections show that deflections increased significantly (60 percent) at all depths in the pavement structure by the end of trafficking.

3.4.6 Permanent Surface Deformation (Rutting)

Figure 3.18 shows the average transverse cross section measured with the Laser Profilometer at various stages of the test and clearly indicates the increase in rutting and deformation over the duration of the test.

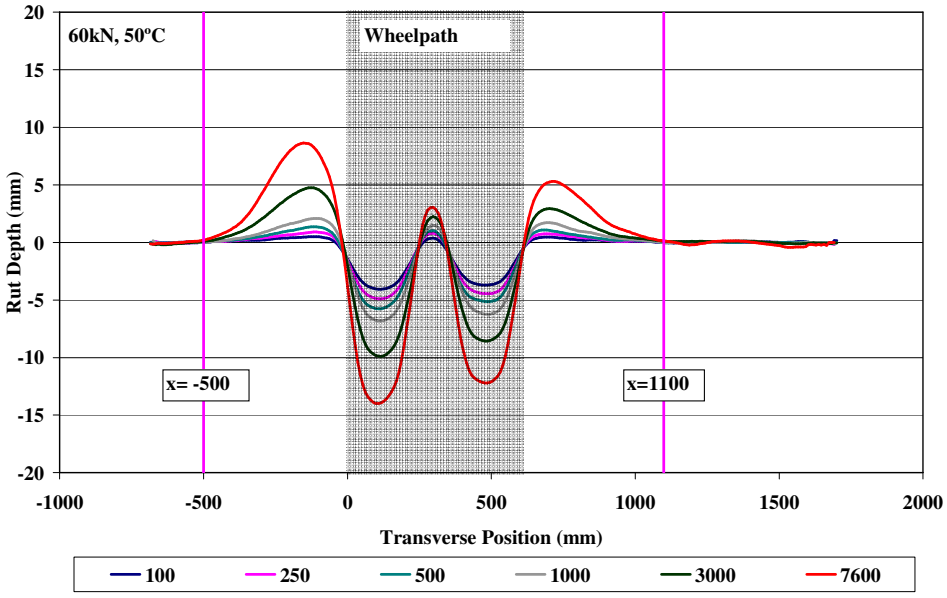

Figure 3.18: 581RF: Profilometer cross section at various load repetitions.

Figures 3.19 and 3.20 show the development of permanent deformation (average maximum rut and average deformation, respectively) with load repetitions as determined by the Laser Profilometer for the test section, with an embedment phase only apparent at the beginning of the experiment. Error bars on the average reading indicate variation along the length of the section. Figure 3.21 shows a contour plot of the pavement surface at the end of the test (7,600 repetitions). After completion of trafficking, the average maximum rut depth and the average deformation were 22.7 mm and 10.3 mm, respectively. The maximum rut depth measured on the section was 27.6 mm. Rut development was rapid with the failure criteria of an average of 12.5 mm total rut depth reached after 2,324 load repetitions.

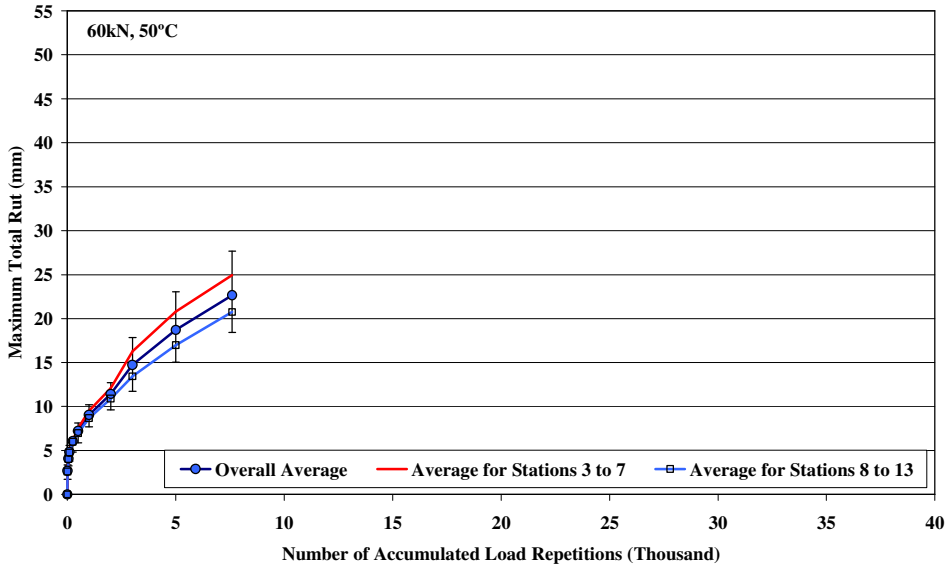

Figure 3.19: 581RF: Average maximum rut.

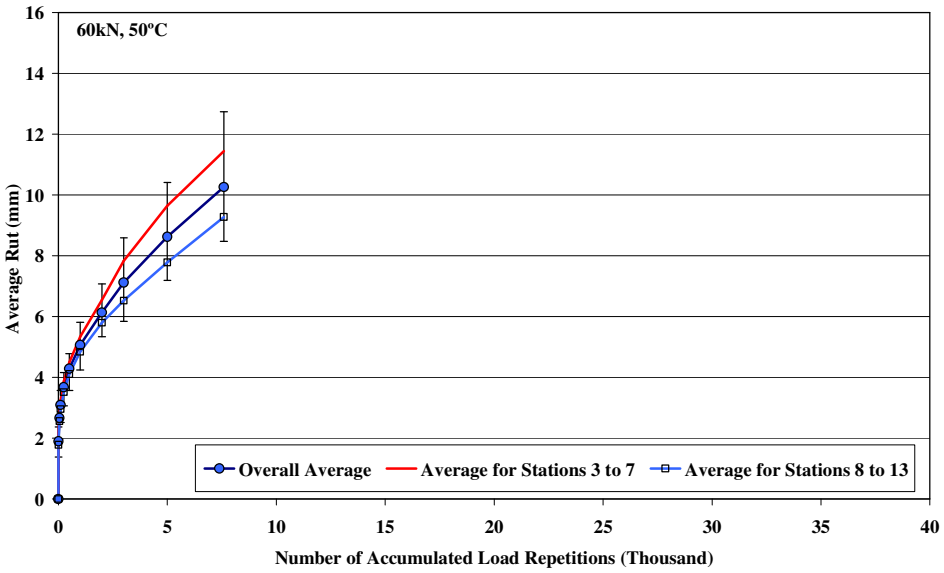

Figure 3.20: 581RF: Average deformation.

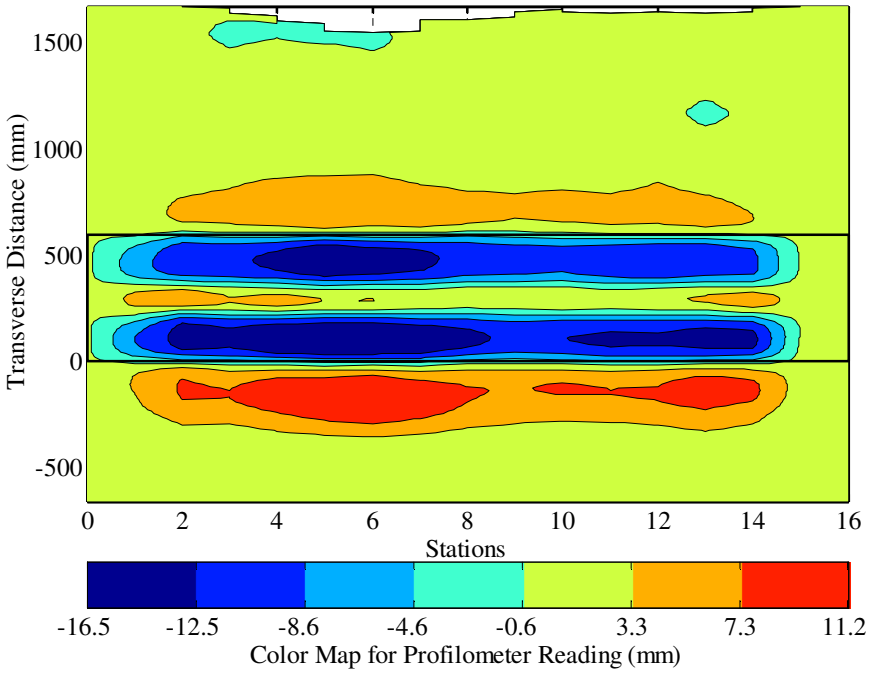

Figure 3.21: 581RF: Contour plot of permanent deformation after 7,600 repetitions.

3.4.7 Permanent In-Depth Deformation

MDD modules were installed at Station 8, at the following depths. A module was not installed on the surface of the overlay due to thickness constraints.

- 120 mm: near the bottom of the underlying DGAC layer
- 325 mm: in the middle of the aggregate base layer
- 530 mm: at the bottom of the aggregate base layer
- 722 mm: 300 mm below the top of the subgrade (not functioning in this test)

Table 3.6 and Figures 3.22 and 3.23 provide an indication of the permanent deformation recorded at MDD8. Figure 3.22 shows the permanent deformation at the MDD modules, while Figure 3.23 shows the permanent deformation calculated for the various layers. The module at the bottom of the asphalt concrete layers started showing upwards (expansive) readings part way through the test. Although the movement was small (0.65 mm), the data for that module is not presented. The data shows that the majority of the permanent deformation occurred in the asphalt concrete layers and the top half of the aggregate base layer (97 percent). However, after excavation and assessment of a test pit it was found that the deformation in the asphalt concrete layers was mostly attributable to the underlying DGAC layer (12). Approximately 4.0 mm of rutting occurred in the overlay and approximately 12 mm in the underlying DGAC. Slight differences between the data obtained from the MDDs and the test pit profile are attributed to their different locations, and to the resolution of measurements on the profile (~1.0 mm).

Table 3.6: 581RF: Vertical Permanent Deformation in Pavement Layers.

Layer	Nominal Thickness (mm)	Vertical Permanent Deformation (mm)	Percentage Total Deformation (%)
AC layers	135	20.6	97.2
Upper aggregate base	205		
Lower aggregate base	205	0.4	1.9
Top 300 mm of subgrade	300	0.2	0.9
Subgrade to anchor	2,158	0.0	0.0
Total (All Layers)	3,000	21.2	100

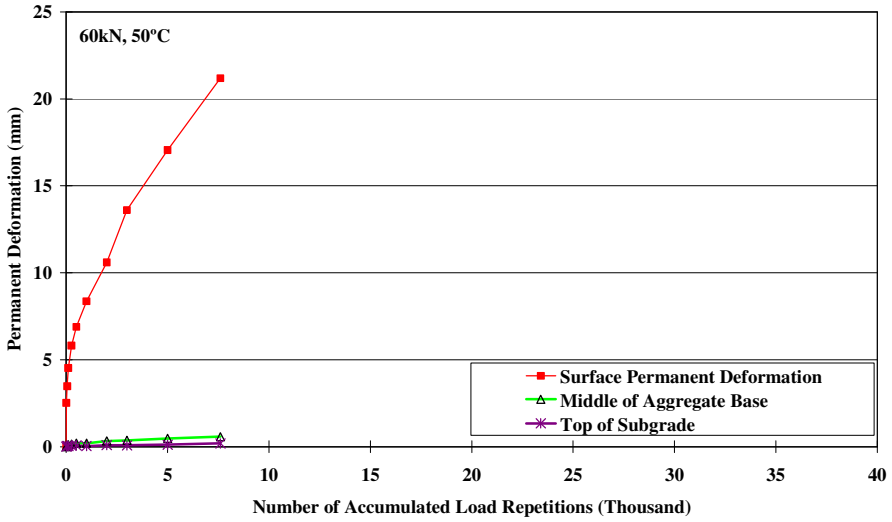

Figure 3.22: 581RF: Permanent in-depth deformation at MDD8.

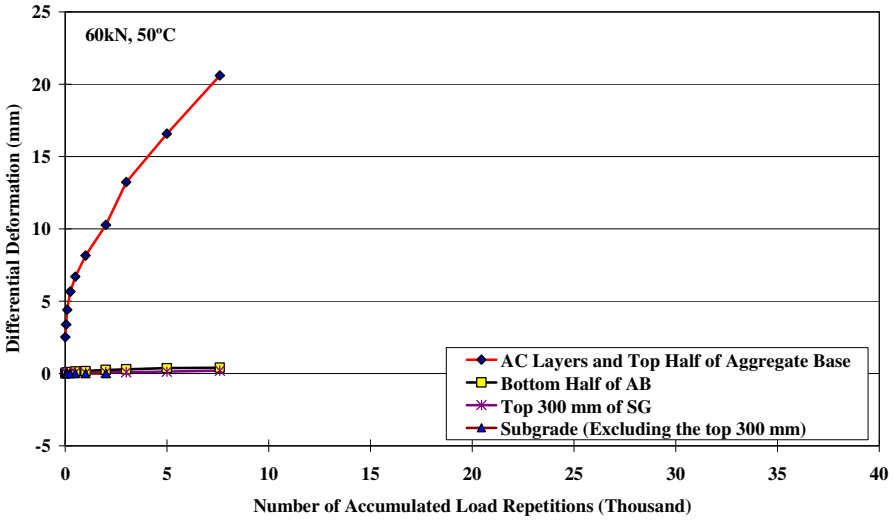

Figure 3.23: 581RF: In-depth differential deformation at MDD8.

3.4.8 Visual Inspection

Apart from rutting, no other distress was recorded on the section. Figure 3.24 shows photographs taken of the surface at the end of the test.

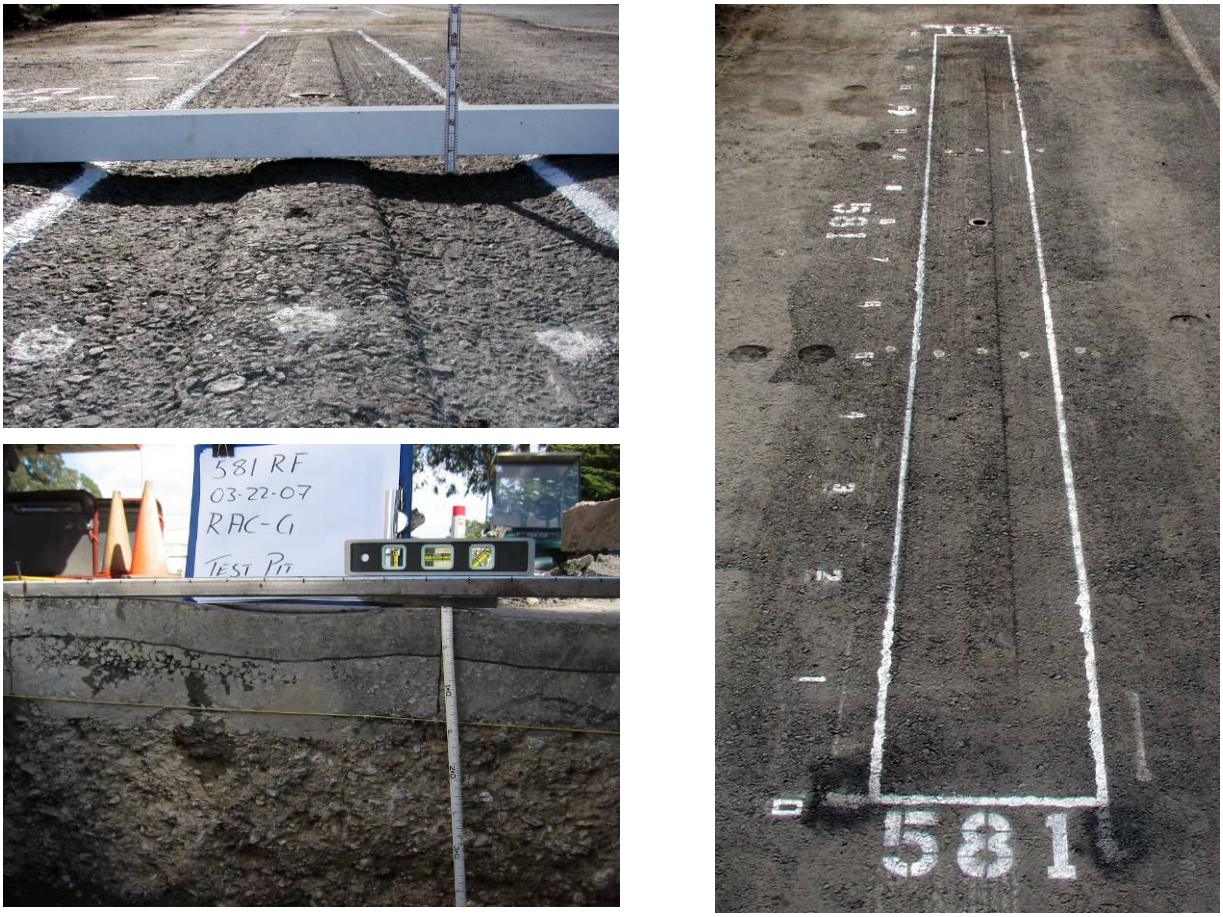

Figure 3.24: 581RF: Section photographs at the end of the test.

3.5. Section 582RF: 90-mm AR4000-D

3.5.1 Test Summary

Loading commenced on September 4, 2003 and ended on September 9, 2003. During this period 18,564 load repetitions were applied and ten datasets were collected.

3.5.2 Air Temperatures in the Temperature Control Unit

Air temperatures inside the temperature control chamber ranged from 50°C to 59°C with an average of 55.3°C and a standard deviation of 1.9°C. Air temperatures were adjusted to maintain a pavement temperature of 50°C±4°C.

The daily average air temperatures recorded in the temperature control unit, calculated from the hourly temperatures recorded during HVS operation, are shown in Figure 3.25. Vertical errors bars on each point on the graph show daily temperature range.

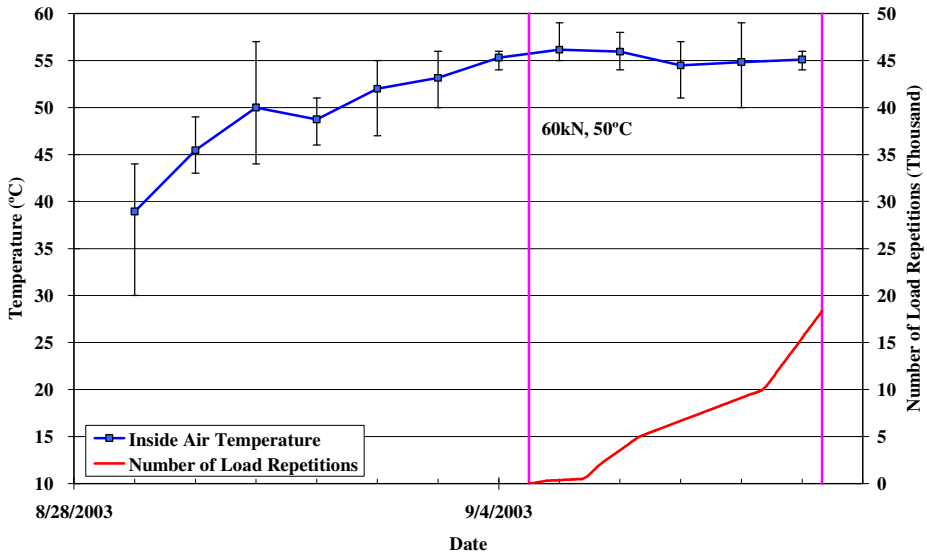

Figure 3.25: 582RF: Daily average air temperatures inside the temperature control chamber.

3.5.3 Outside Air Temperatures

Outside air temperatures ranged from 12°C to 29°C with an average of 17.1°C and are summarized in Figure 3.26. Vertical error bars on each point on the graph show daily temperature range.

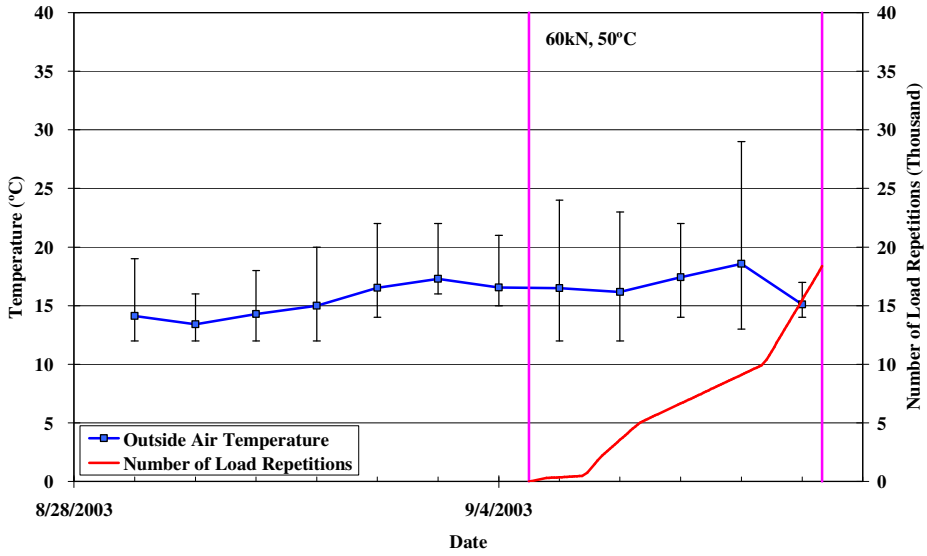

Figure 3.26: 582RF: Daily average air temperatures outside the temperature control chamber.

3.5.4 Temperatures in the Asphalt Concrete Layer

Daily averages of the surface and in-depth temperatures are listed in Table 3.7 and shown in Figure 3.27. Pavement temperatures decreased slightly with increasing depth in the pavement.

Table 3.7: 582RF: Temperature Summary for Air and Pavement.

Temperature	Average (°C)	Std Dev (°C)
Outside air	17.1	3.4
Inside air	55.3	1.9
Pavement surface	50.4	3.0
- 25 mm below surface	49.3	2.6
- 50 mm below surface	48.2	2.2
- 90 mm below surface	47.3	2.0
- 120 mm below surface	43.1	7.8

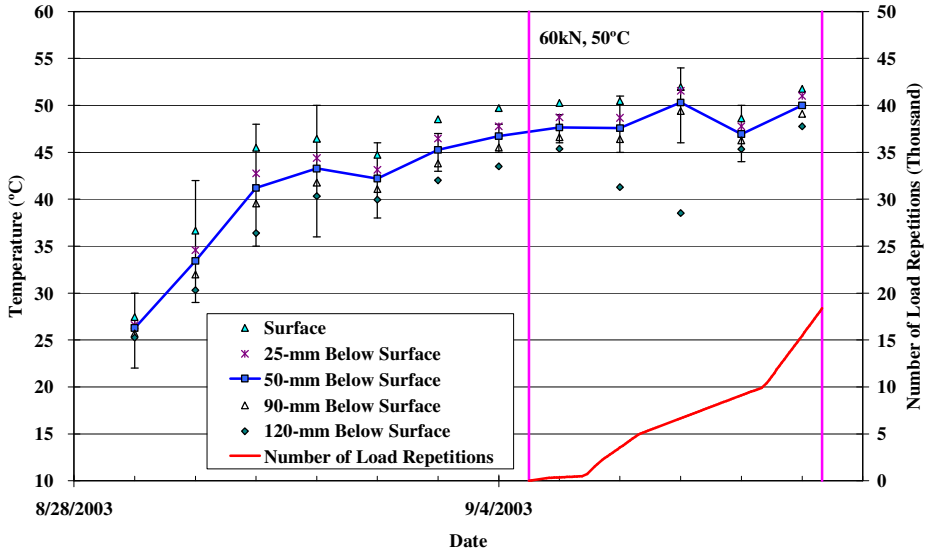

Figure 3.27: 582RF: Daily average temperatures at pavement surface and various depths.

3.5.5 In-Depth Elastic Deflection from MDD

In-depth elastic deflection measurements were taken from the MDD module with a test load of 60 kN at various times during trafficking. Table 3.8 and Figure 3.28 summarize the in-depth elastic deflections measured at various depths with MDD8.

Table 3.8: 582RF: Summary of 60 kN In-Depth Elastic Deflections.

Depth (mm)	Layer	Elastic Deflection at 60 kN (microns)		
		Before Trafficking	After Trafficking	Ratio of Final/Initial
195	Bottom of underlying DGAC	0.633	0.839	1.33
400	Middle of aggregate base	0.486	0.652	1.34
605	Bottom of aggregate base	0.368	0.500	1.36

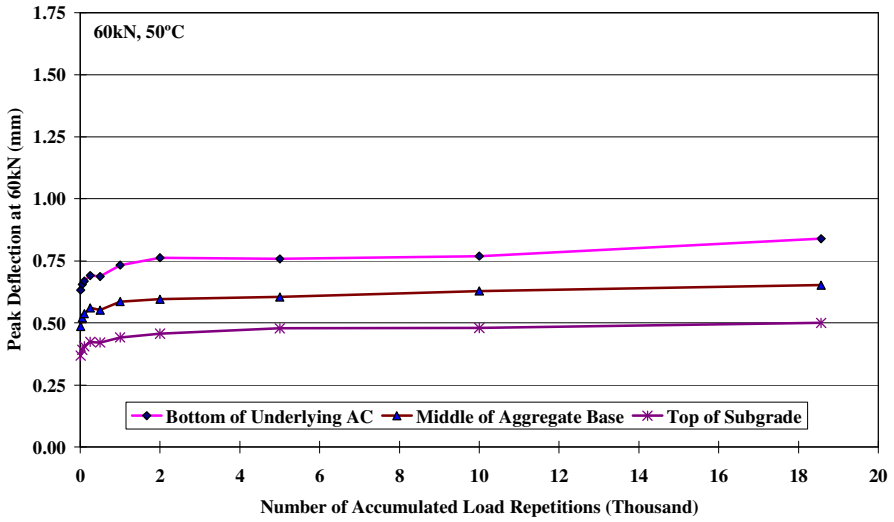

Figure 3.28: 582RF: Elastic deflections at MDD8 with 60 kN test load.

The following observations were made from the data collected:

- The elastic deflections increased slightly at the beginning of the experiment, which is typical.
- The effect of trafficking load on elastic deformation decreased with increasing depth, as expected. Most of the damage observed appeared to occur in the upper portion of the pavement, which was verified in a forensic investigation (12).
- Ratios of final-to-initial MDD deflections show that deflections increased (34 percent) at all depths in the pavement structure by the end of trafficking.

3.5.6 Permanent Surface Deformation (Rutting)

Figure 3.29 shows the average transverse cross section measured with the Laser Profilometer at various stages of the test and clearly shows the increase in rutting and deformation over the duration of the test.

Figures 3.30 and 3.31 show the development of permanent deformation (average maximum rut and average deformation, respectively) with load repetitions as determined by the Laser Profilometer for the test section, with an embedment phase only apparent at the beginning of the experiment. Error bars on the average reading indicate variation along the length of the section. Figure 3.32 shows a contour plot of the pavement surface at the end of the test (18,564 repetitions). After completion of trafficking, the average maximum rut depth and the average deformation were 15.6 mm and 8.1 mm, respectively. The maximum rut depth measured on the section was 20.0 mm. Rut development was rapid with the failure criteria of an average of 12.5 mm total rut depth reached after 8,266 load repetitions.

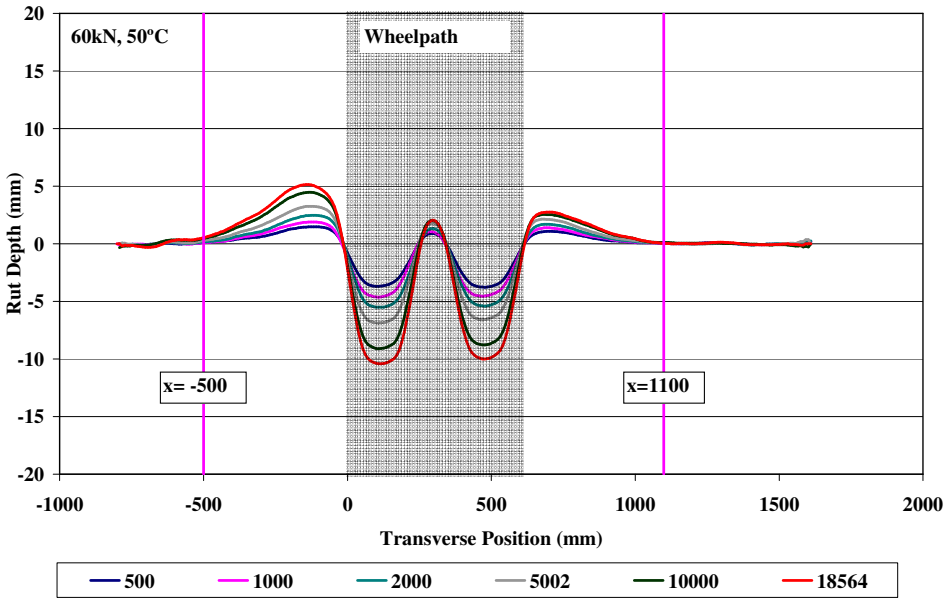

Figure 3.29: 582RF: Profilometer cross section at various load repetitions.

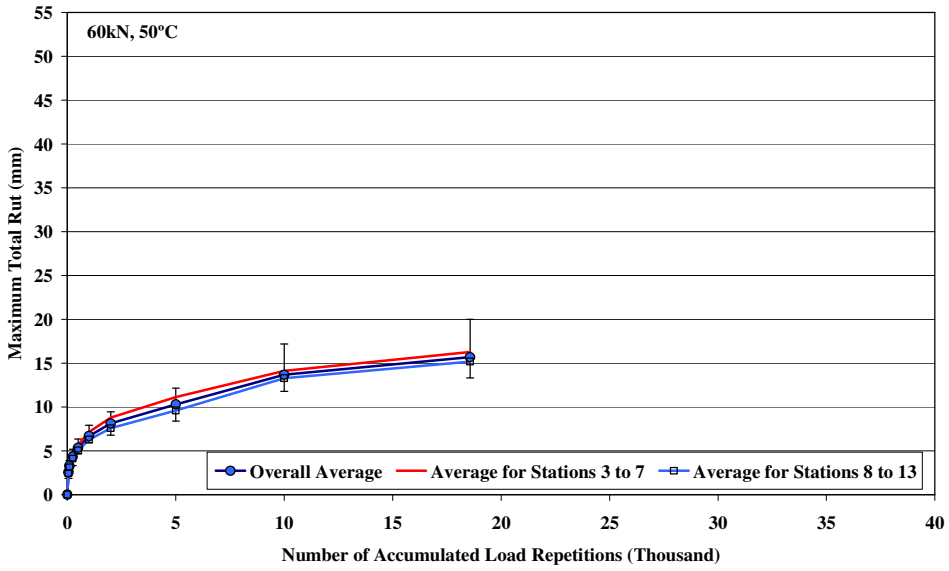

Figure 3.30: 582RF: Average maximum rut.

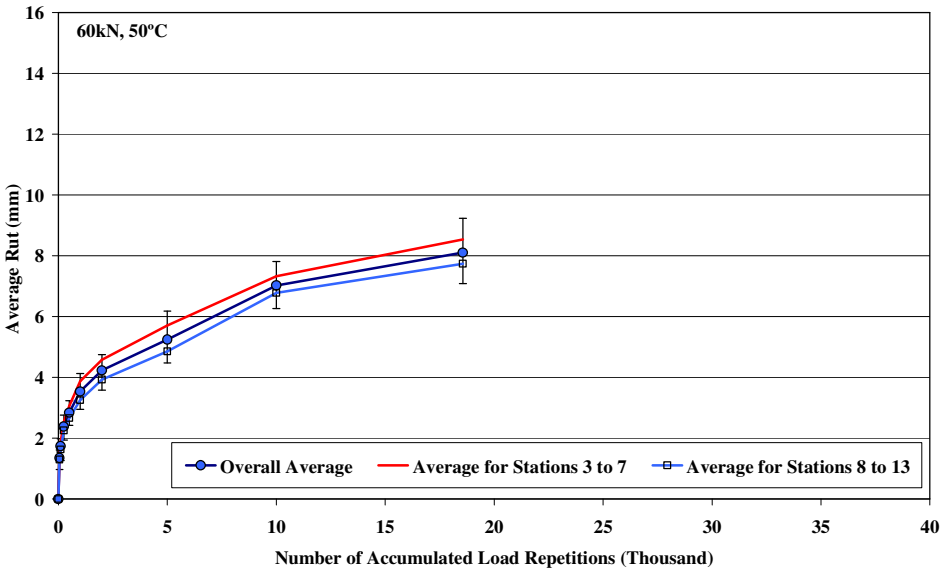

Figure 3.31: 582RF: Average deformation.

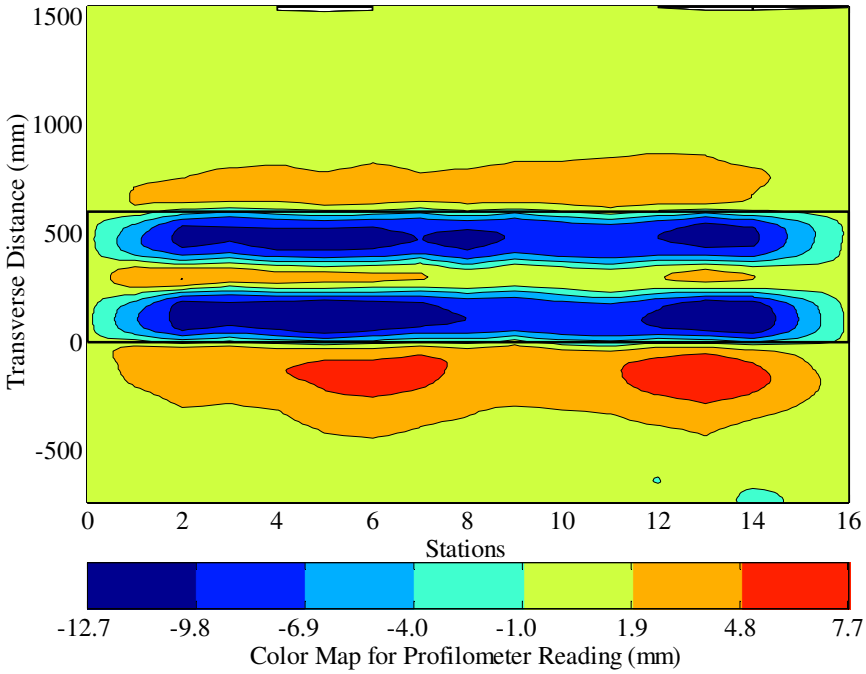

Figure 3.32: 582RF: Contour plot of permanent deformation after 18,564 repetitions.

3.5.7 Permanent In-Depth Deformation

Permanent in-depth deformation was measured with MDD modules installed at Station 8, at the following depths. A module was not installed on the surface of the overlay due to thickness constraints.

- 195 mm: near the bottom of the underlying DGAC layer
- 400 mm: in the middle of the aggregate base layer
- 605 mm: at the bottom of the aggregate base layer
- 922 mm: 300 mm below the top of the subgrade (not functioning in this test)

Table 3.9 and Figures 3.33 and 3.34 provide an indication of the permanent deformation recorded at MDD8. Figure 3.33 shows the permanent deformation at the MDD modules, while Figure 3.34 shows the permanent deformation calculated for the various layers. The data shows that the majority of the permanent deformation occurred in the asphalt concrete layers (94 percent). This was verified during an assessment of a test pit, which found that the deformation was almost equally attributable to both DGAC layers (12). Approximately 3.0 mm of rutting occurred in the overlay and approximately 5 mm occurred in the underlying DGAC. Slight differences between the data obtained from the MDDs and the test pit were attributed to the different locations of the MDD and test pit profile, and the resolution of measurements on the profile (~1.0 mm).

Table 3.9: 582RF: Vertical Permanent Deformation in Pavement Layers.

Layer	Nominal Thickness (mm)	Vertical Permanent Deformation (mm)	Percentage Total Deformation (%)
AC layers	180	13.1	93.9
Upper aggregate base	205	0.3	2.3
Lower aggregate base	205	0.4	3.2
Top 300 mm of subgrade	300	13.1	0.6
Subgrade to anchor	2,158		
Total (All Layers)	3,000	22.2	100

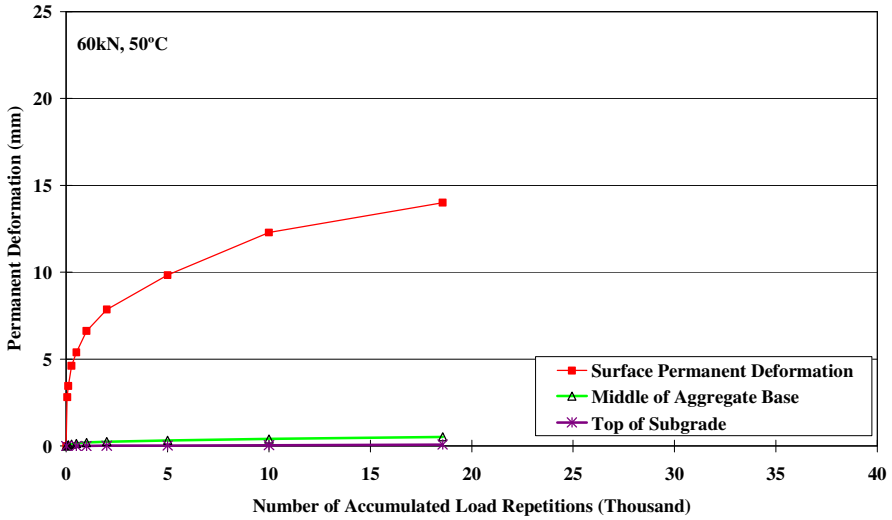

Figure 3.33: 582RF: Permanent in-depth deformation at MDD8.

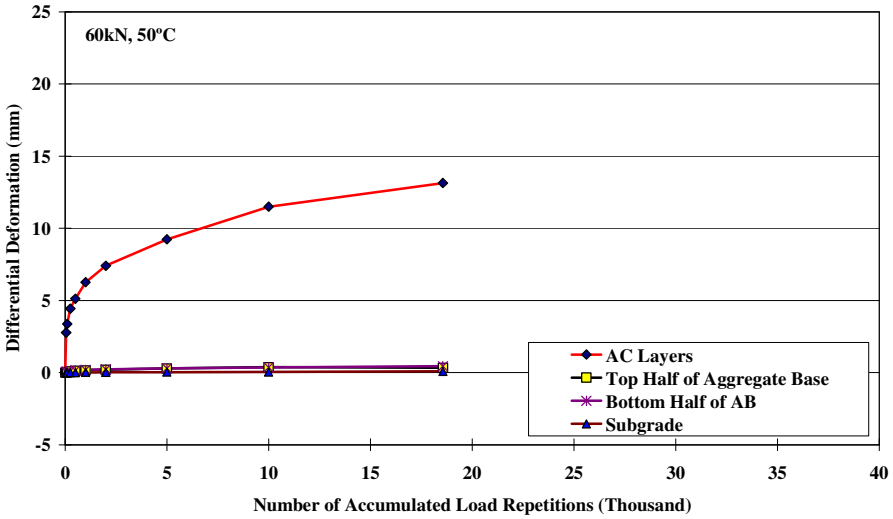

Figure 3.34: 582RF: In-depth differential deformation at MDD8.

3.5.8 Visual Inspection

Apart from rutting, no other distress was recorded on the section. Figure 3.35 shows photographs taken of the surface at the end of the test.

Figure 3.35: 582RF: Section photographs at the end of the test.

3.6. Section 583RF: 45 mm MB4-G

3.6.1 Test Summary

Loading commenced on December 8, 2003 and ended on December 16, 2003. During this period 15,000 load repetitions were applied and ten datasets were collected.

3.6.2 Air Temperatures in the Temperature Control Unit

Air temperatures inside the temperature control chamber ranged from 41°C to 57°C, with an average of 49°C and a standard deviation of 3.9°C. Air temperatures were adjusted to maintain a pavement temperature of 50°C±4°C. The daily average air temperatures recorded in the temperature control unit, calculated from the hourly temperatures recorded during HVS operation, are shown in Figure 3.36. Vertical errors bars on each point on the graph show daily temperature range.

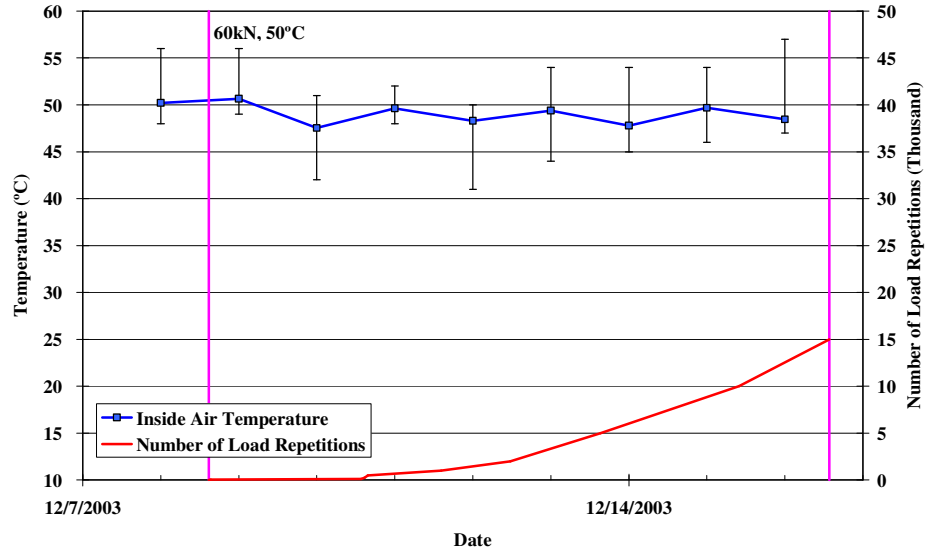

Figure 3.36: 583RF: Daily average air temperatures inside the temperature control chamber.

3.6.3 Outside Air Temperatures

Outside air temperatures ranged from 4°C to 18°C with an average of 10.6°C and are summarized in Figure 3.37. Vertical error bars on each point on the graph show daily temperature range.

3.6.4 Temperatures in the Asphalt Concrete Layer

Daily averages of the surface and in-depth temperatures are listed in Table 3.10 and shown in Figure 3.38. Pavement temperatures decreased slightly with increasing depth in the pavement.

Table 3.10: 583RF: Temperature Summary for Air and Pavement.

Temperature	Average (°C)	Std Dev (°C)
Outside air	10.6	3.0
Inside air	49.1	3.9
Pavement surface	51.8	3.8
- 25 mm below surface	50.3	3.3
- 50 mm below surface	48.4	2.8
- 90 mm below surface	47.4	2.7
- 120 mm below surface	46.3	2.5

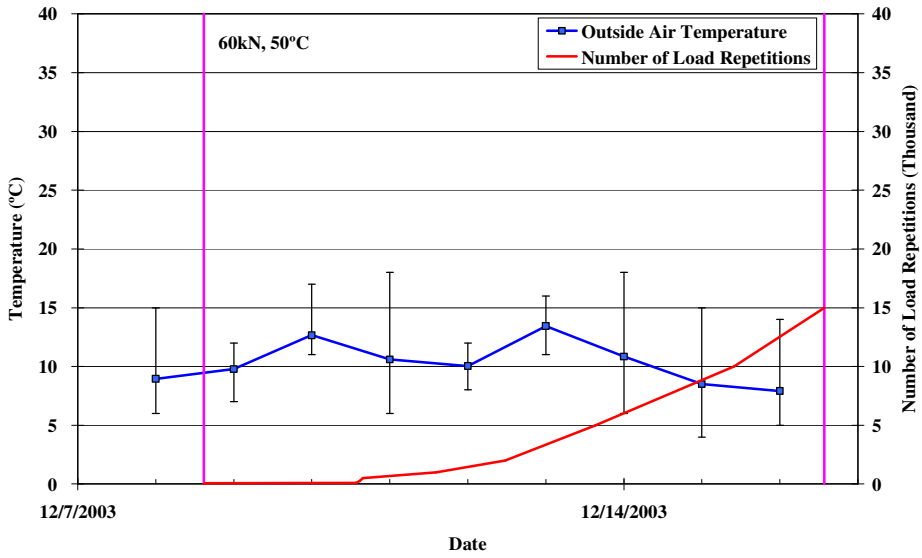

Figure 3.37: 583RF: Daily average air temperatures outside the temperature control chamber.

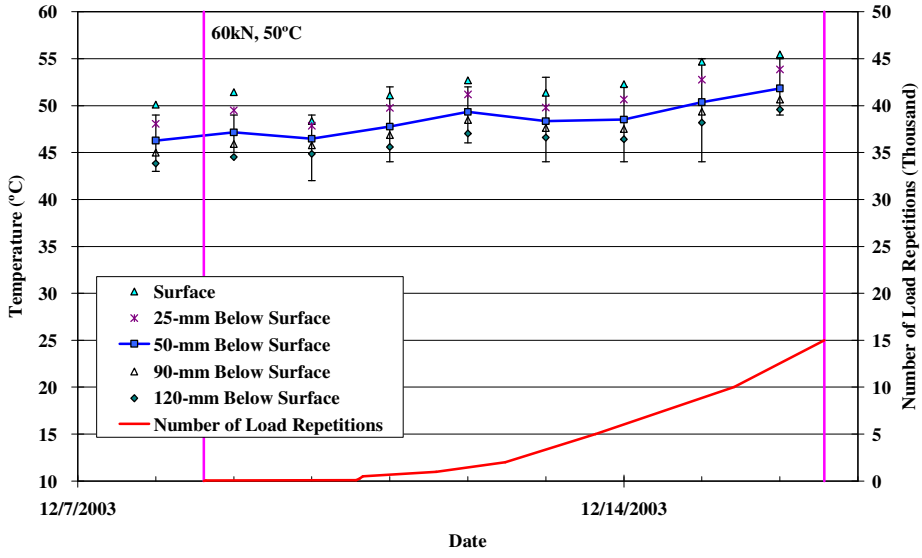

Figure 3.38: 583RF: Daily average temperatures at pavement surface and various depths.

3.6.5 In-Depth Elastic Deflection from MDD

In-depth elastic deflection measurements were made with a test load of 60 kN at various times during trafficking. Table 3.11 and Figure 3.39 summarize the in-depth elastic deflections measured at various depths with MDD8.

Table 3.11: 583RF: Summary of 60 kN In-Depth Elastic Deflections.

Depth (mm)	Layer	Elastic Deflection at 60 kN (microns)		
		Before Trafficking	After Trafficking	Ratio of Final/Initial
132	Bottom of underlying DGAC	0.445	0.562	1.26
337	Middle of aggregate base	0.329	0.346	1.05
542	Bottom of aggregate base	0.239	0.243	1.02
842	300 mm below top of subgrade	0.143	0.133	0.93

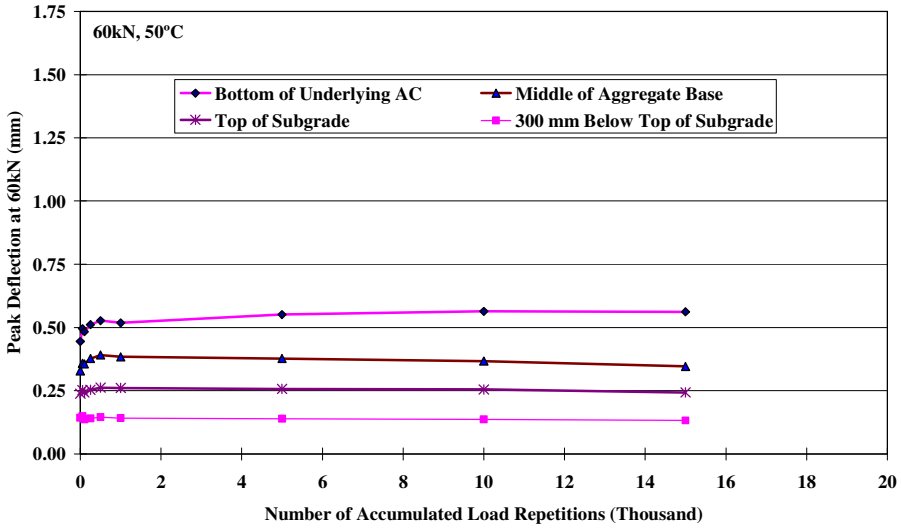

Figure 3.39: 583RF: Elastic deflections at MDD8 with 60 kN test load.

The following observations were made from the data collected:

- The elastic deflections increased slightly at the beginning of the experiment.
- The effect of trafficking load on elastic deformation decreased with increasing depth, as expected. Most of the damage observed appeared to occur in the upper portion of the pavement, which was verified in a forensic investigation (12).
- Ratios of final-to-initial MDD deflections show that deflections increased (between 2 and 26 percent) at all depths in the pavement structure by the end of trafficking.

3.6.6 Permanent Surface Deformation (Rutting)

Figure 3.40 shows the average transverse cross section measured with the Laser Profilometer at various stages of the test and clearly shows the increase in rutting and deformation over the duration of the test.

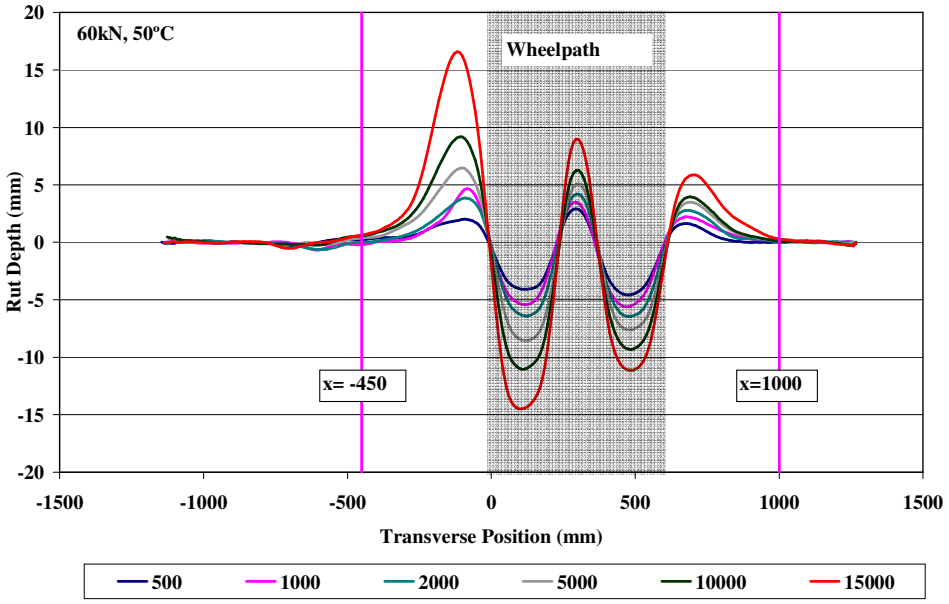

Figure 3.40: 583RF: Profilometer cross section at various load repetitions.

Figures 3.41 and 3.42 show the development of permanent deformation (average maximum rut and average deformation, respectively) with load repetitions as determined by the Laser Profilometer for the test section, with an embedment phase only apparent at the beginning of the experiment. Error bars on the average reading indicate variation along the length of the section. Figure 3.43 shows a contour plot of the pavement surface at the end of the test (15,000 repetitions). After completion of trafficking, the average maximum rut depth and the average deformation were 31.3 mm and 9.7 mm, respectively. The maximum rut depth measured on the section was 54.3 mm. Rut development was gradual with the failure criteria of an average of 12.5 mm total rut depth reached after 3,043 load repetitions.

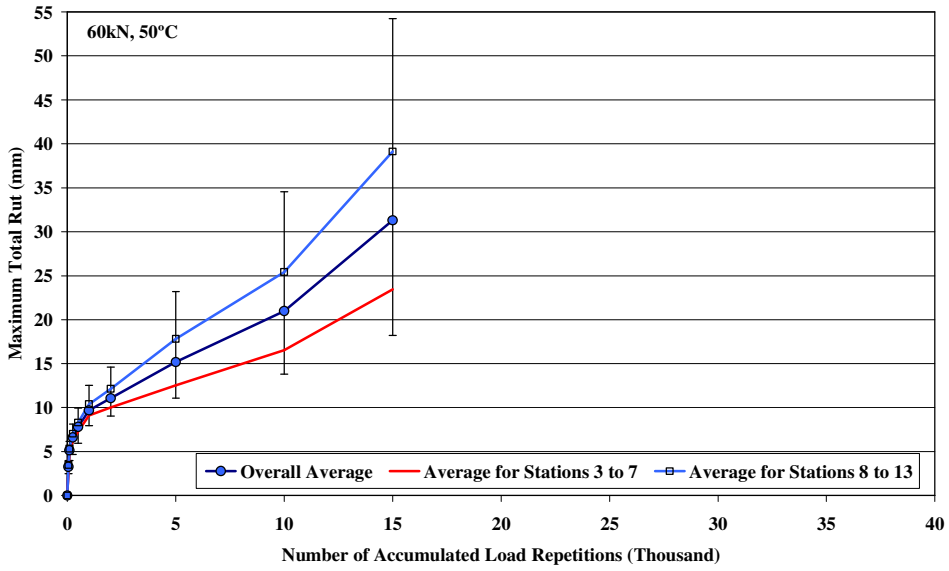

Figure 3.41: 583RF: Average maximum rut.

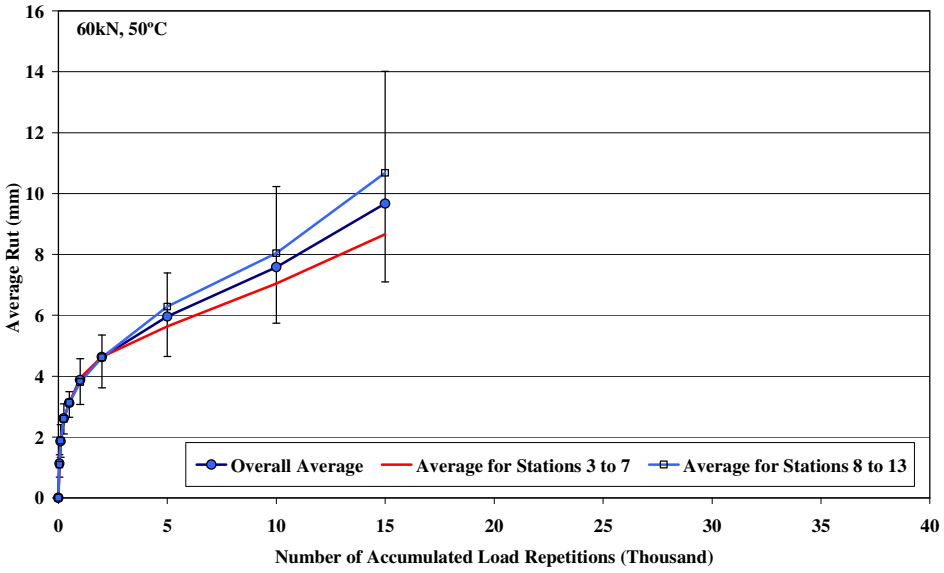

Figure 3.42: 583RF: Average deformation.

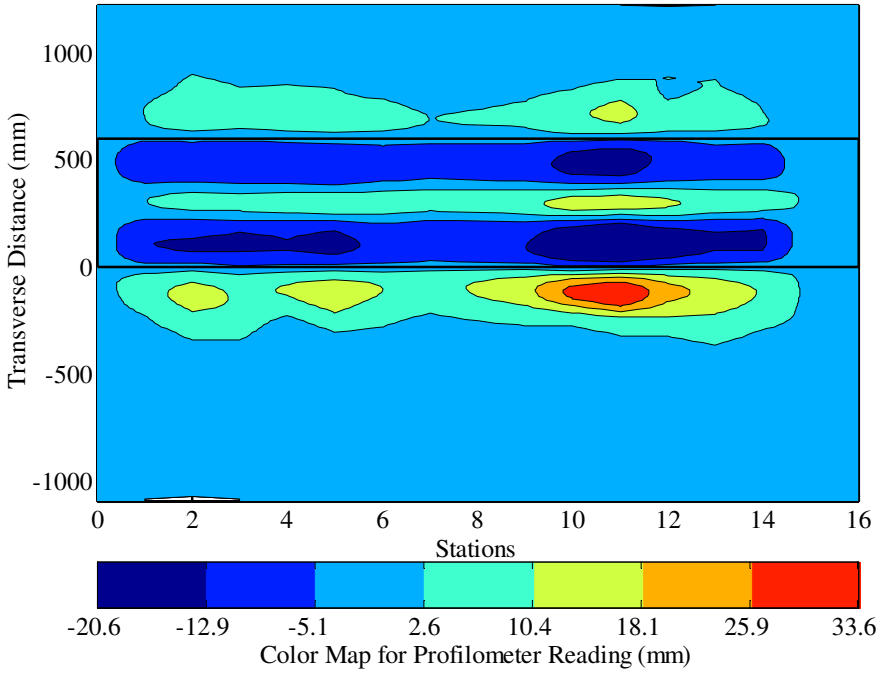

Figure 3.43: 583RF: Contour plot of permanent deformation after 15,000 repetitions.

3.6.7 Permanent In-Depth Deformation

Permanent in-depth deflection was measured from MDD modules installed at Station 8, at the following depths. A module was not installed on the surface of the overlay due to thickness constraints.

- 132 mm: near the bottom of the underlying DGAC layer
- 337 mm: in the middle of the aggregate base layer
- 542 mm: at the bottom of the aggregate base layer
- 842 mm: 300 mm below the top of the subgrade

Table 3.12 and Figures 3.44 and 3.45 provide an indication of the permanent deformation recorded at MDD8. Figure 3.44 shows the permanent deformation at the MDD modules, while Figure 3.45 shows the permanent deformation calculated for the various layers. The data indicates that the majority of the permanent deformation occurred in the asphalt concrete layers (98 percent). This was verified in a forensic investigation, which showed the deformation was almost completely attributable to the underlying DGAC layer (12). Approximately 1.0 mm of rutting occurred in the overlay and approximately 6.0 mm occurred in the underlying DGAC. A substantial amount of shoving occurred between Stations 10 through 12, where the split in rutting between the overlay and the underlying DGAC was 20/80 percent. Slight differences between the data obtained from the MDDs and the test pits are attributed to the different locations of the MDD and test pit profile, and the resolution of the profile measurements (~1.0 mm).

Table 3.12: 583RF: Vertical Permanent Deformation in Pavement Layers.

Layer	Nominal Thickness (mm)	Vertical Permanent Deformation (mm)	Percentage Total Deformation (%)
AC layers	135	17.9	98.2
Upper aggregate base	205	0.2	1.2
Lower aggregate base	205	0.1	0.7
Top 300 mm of subgrade	300	0.1	0.4
Subgrade to anchor	2,158	-0.1	-0.5
Total (All Layers)	3,000	18.2	100

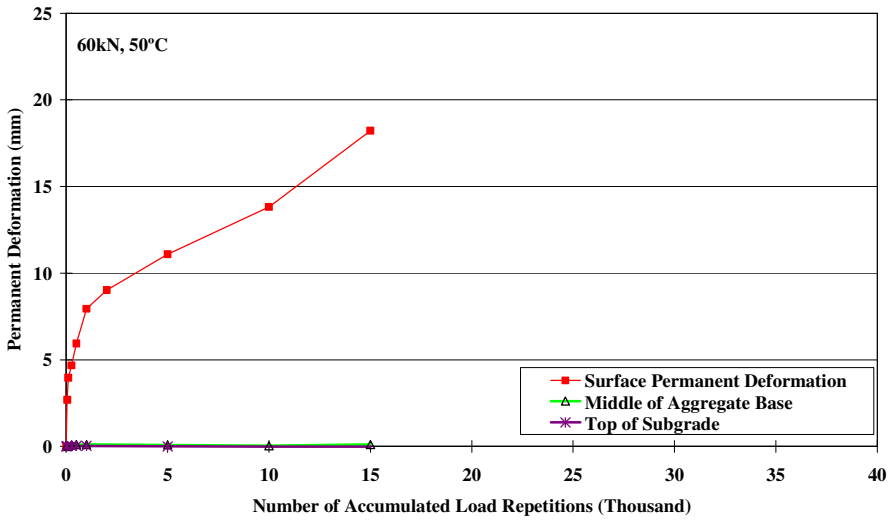

Figure 3.44: 583RF: Permanent in-depth deformation at MDD8.

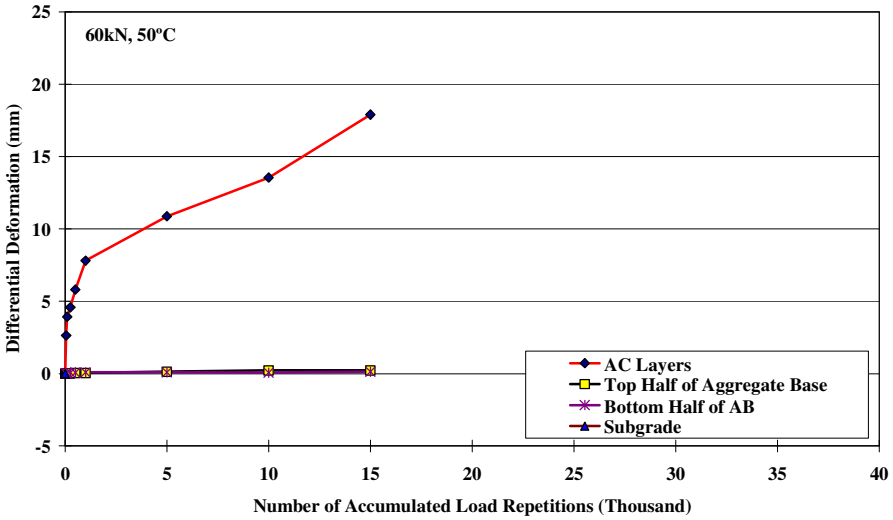

Figure 3.45: 583RF: In-depth differential deformation at MDD8.

3.6.8 Visual Inspection

Apart from rutting, no other distress was recorded on the section. Figure 3.46 shows photographs taken of the surface at the end of the test.

Figure 3.46: 583RF: Section photographs at the end of the test.

3.7. Section 584RF: 90 mm MB4-G

3.7.1 Test Summary

Loading commenced on November 13, 2003 and ended on November 26, 2003. During this period 34,800 load repetitions were applied and eleven datasets were collected.

3.7.2 Air Temperatures in the Temperature Control Unit

Air temperatures inside the temperature control chamber ranged from 33°C to 56°C with an average of 49°C and standard deviation of 4.5°C. Air temperatures were adjusted to maintain a pavement temperature of 50°C±4°C.

The daily average air temperatures recorded in the temperature control unit, calculated from the hourly temperatures recorded during HVS operation, are shown in Figure 3.47. Vertical errors bars on each point on the graph show daily temperature range.

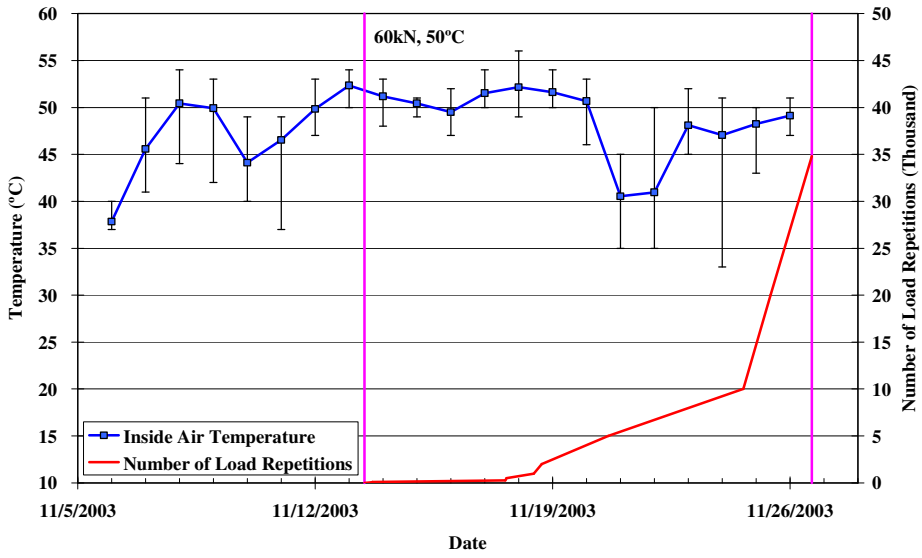

Figure 3.47: 584RF: Daily average air temperatures inside the temperature control chamber.

3.7.3 Outside Air Temperatures

Outside air temperatures ranged from 3°C to 23°C with an average of 11.1°C and are summarized in Figure 3.48. Vertical error bars on each point on the graph show daily temperature range.

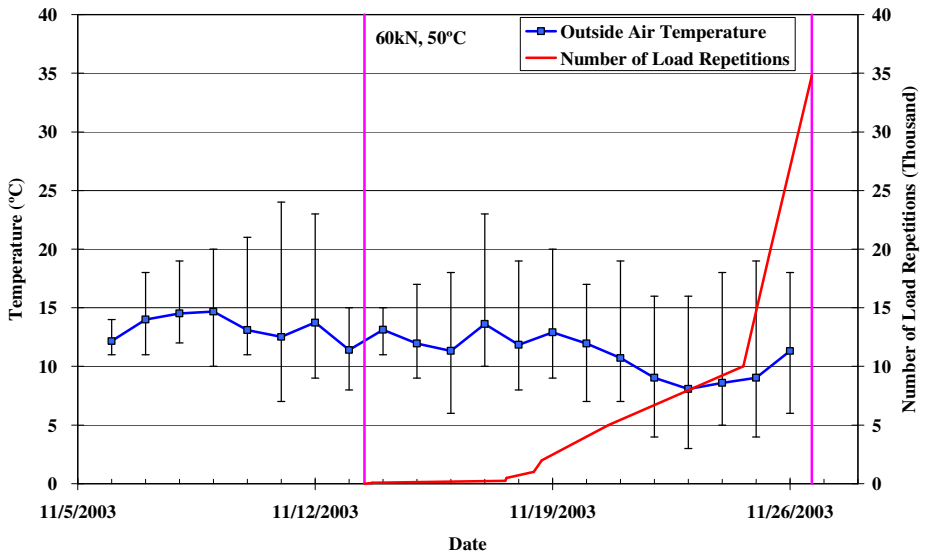

Figure 3.48: 584RF: Daily average air temperatures outside the temperature control chamber.

3.7.4 Temperatures in the Asphalt Concrete Layer

Daily averages of the surface and in-depth temperatures are listed in Table 3.13 and shown in Figure 3.49. Pavement temperatures decreased slightly with increasing depth in the pavement.

Table 3.13: 584RF: Temperature Summary for Air and Pavement.

Temperature	Average (°C)	Std Dev (°C)
Outside air	11.1	3.9
Inside air	48.5	4.5
Pavement surface	50.9	3.5
- 25 mm below surface	50.6	3.4
- 50 mm below surface	49.1	3.2
- 90 mm below surface	48.2	3.0
- 120 mm below surface	47.3	2.9

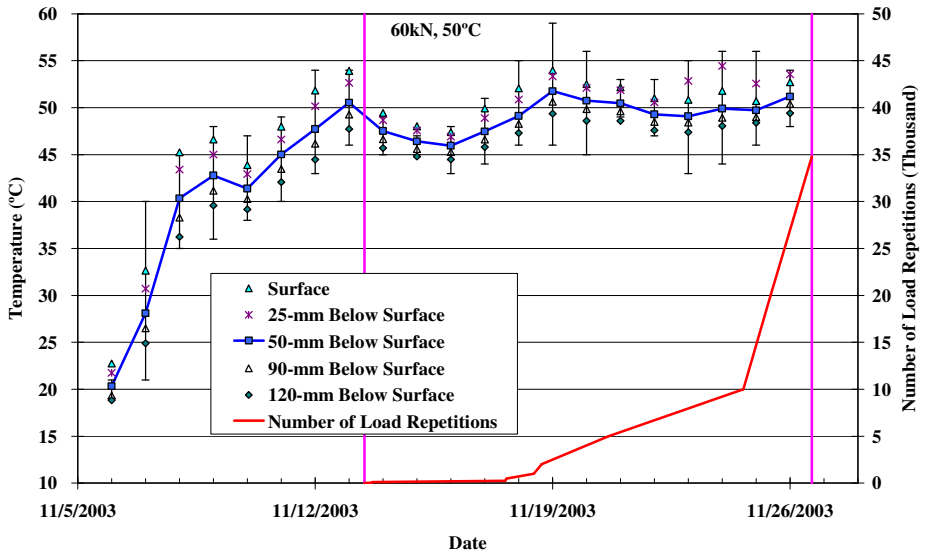

Figure 3.49: 584RF: Daily average temperatures at pavement surface and various depths.

3.7.5 In-Depth Elastic Deflection from MDD

In-depth elastic deflection measurements were made with a test load of 60 kN at various times during trafficking. Table 3.14 and Figure 3.50 summarize the in-depth elastic deflections measured at various depths with MDD8.

Table 3.14: 584RF: Summary of 60 kN In-Depth Elastic Deflections.

Depth (mm)	Layer	Elastic Deflection at 60 kN (microns)		
		Before Trafficking	After Trafficking	Ratio of Final/Initial
158	Bottom of underlying DGAC	0.737	0.802	1.09
363	Middle of aggregate base	0.593	0.777	1.31
568	Bottom of aggregate base	0.455	0.579	1.27
868	300 mm below top of subgrade	0.228	0.270	1.18

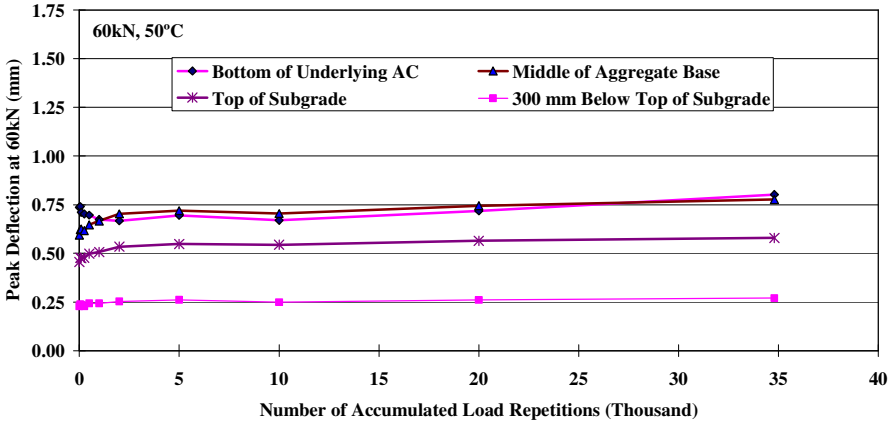

Figure 3.50: 584RF: Elastic deflections at MDD8 with 60 kN test load.

The following observations were made from the data collected:

- The elastic deflections increased slightly at the beginning of the experiment.
- The effect of trafficking load on elastic deformation decreased with increasing depth, as expected. Most of the damage observed appeared to occur in the upper portion of the pavement, which was verified in a forensic investigation after testing (12).
- Ratios of final-to-initial MDD deflections show that deflections increased (between 9 and 31 percent) at all depths in the pavement structure by the end of trafficking.

3.7.6 Permanent Surface Deformation (Rutting)

Figure 3.51 shows the average transverse cross section measured with the Laser Profilometer at various stages of the test and clearly shows the increase in rutting and deformation over the duration of the test.

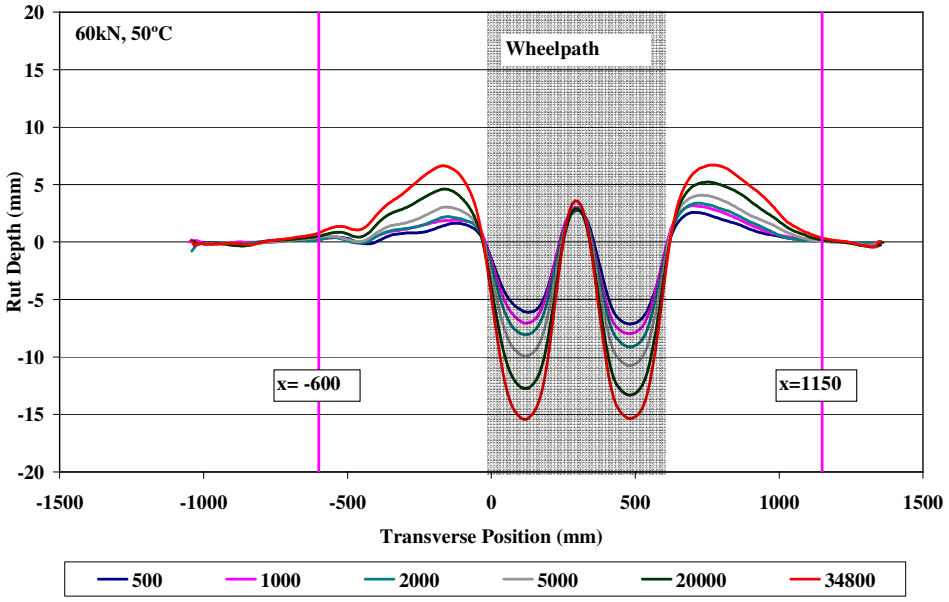

Figure 3.51: 584RF: Profilometer cross section at various load repetitions.

Figures 3.52 and 3.53 show the development of permanent deformation (average maximum rut and average deformation, respectively) with load repetitions as determined by the Laser Profilometer for the test section, with an embedment phase only apparent at the beginning of the experiment. Error bars on the average reading indicate variation along the length of the section. Figure 3.54 shows a contour plot of the pavement surface at the end of the test (34,800 repetitions). After completion of trafficking, the average maximum rut depth and the average deformation were 23.3 mm and 11.9 mm, respectively. The maximum rut depth measured on the section was 29.7 mm. Rut development was rapid with the failure criteria of an average of 12.5 mm total rut depth reached after 1,522 load repetitions.

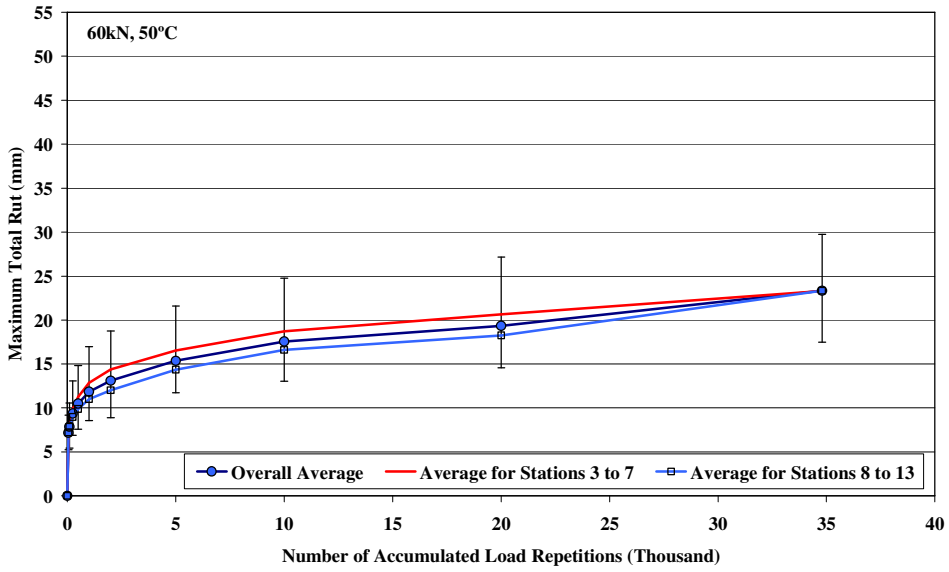

Figure 3.52: 584RF: Average maximum rut.

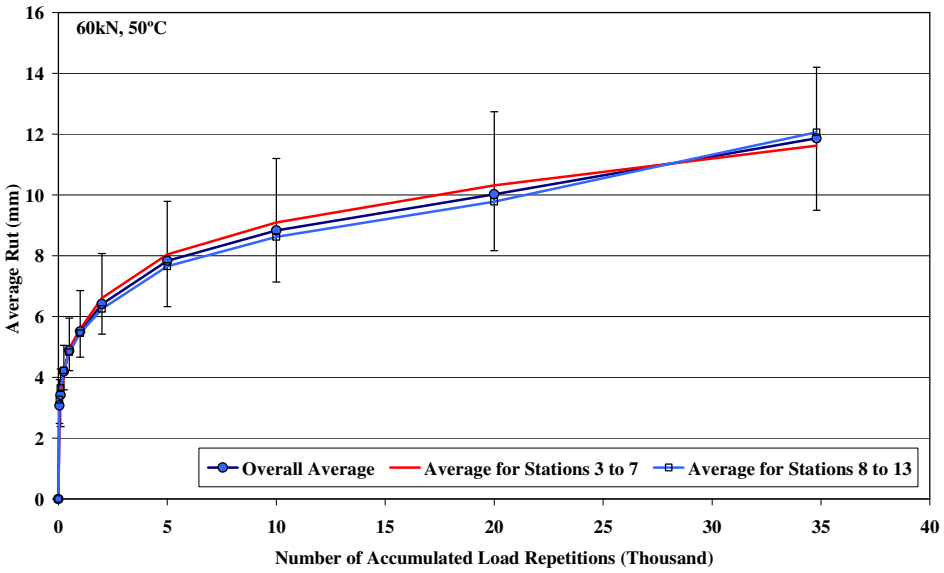

Figure 3.53: 584RF: Average deformation.

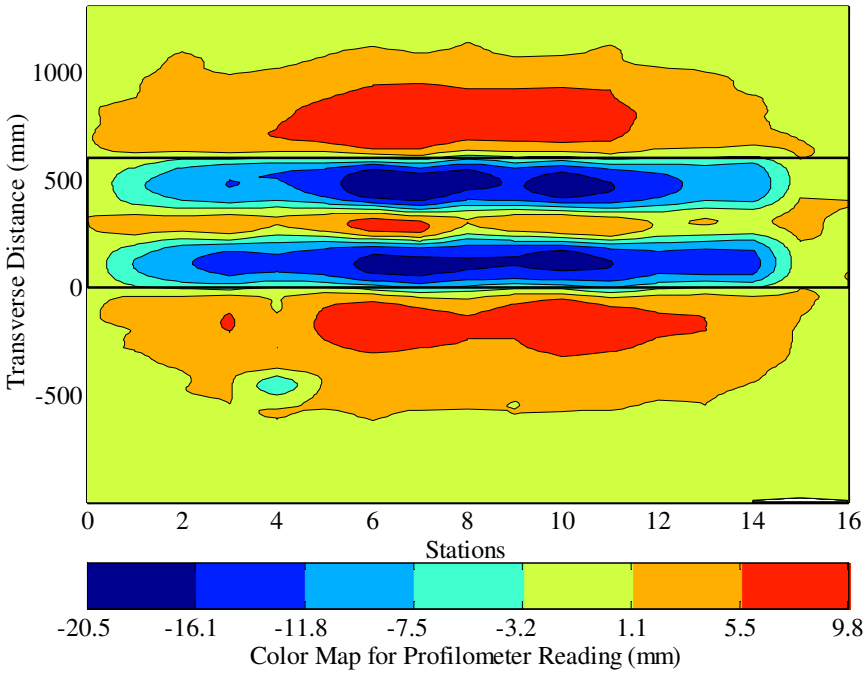

Figure 3.54: 584RF: Contour plot of permanent deformation after 34,800 repetitions.

3.7.7 Permanent In-Depth Deformation

Permanent in-depth deformation was measured with MDD modules installed at Station 8, at the following depths. A module was not installed on the surface of the overlay due to thickness constraints.

- 158 mm: near the bottom of the underlying DGAC layer
- 363 mm: in the middle of the aggregate base layer
- 568 mm: at the bottom of the aggregate base layer
- 868 mm: 300 mm below the top of the subgrade

Table 3.15 and Figures 3.55 and 3.56 provide an indication of the permanent deformation recorded at MDD8. Figure 3.55 shows the permanent deformation at the MDD modules, while Figure 3.56 shows the permanent deformation calculated for the various layers. The data shows that almost all the permanent deformation occurred in the asphalt concrete layers (99 percent). This was verified in a forensic investigation (12), which found that the deformation in the asphalt concrete was equally attributable to both layers. Approximately 8.0 mm of rutting occurred in the overlay and approximately 6.0 mm in the underlying DGAC. Slight differences between the data obtained from the MDDs and the test pit are attributed to the different locations of the MDD and profile, and the resolution of the profile measurements (~1.0 mm).

Table 3.15: 584RF: Vertical Permanent Deformation in Pavement Layers.

Layer	Nominal Thickness (mm)	Vertical Permanent Deformation (mm)	Percentage Total Deformation (%)
AC layers	135	24.1	100.2
Upper aggregate base	205	0.4	1.7
Lower aggregate base	205	-0.2	-1.0
Top 300 mm of subgrade	300	-0.3	-1.5
Subgrade to anchor	2,158	0.1	0.6
Total (All Layers)	3,000	24.0	100

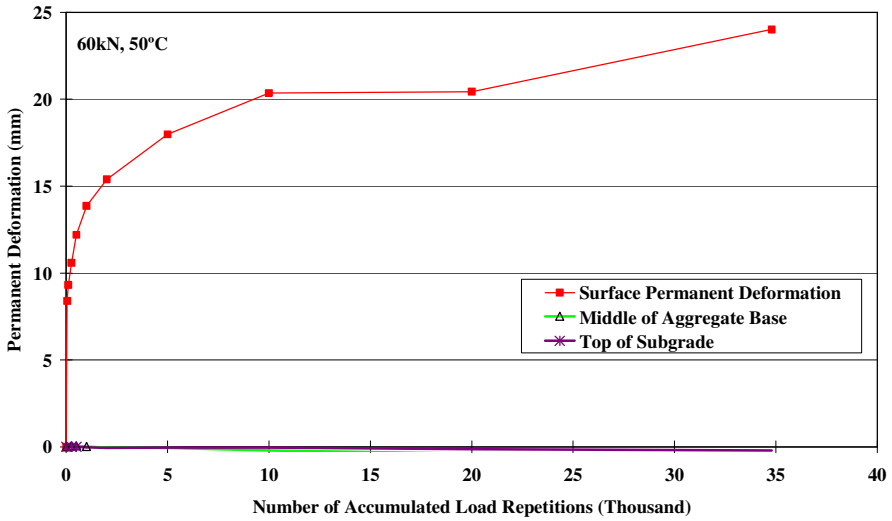

Figure 3.55: 584RF: Permanent in-depth deformation at MDD8.

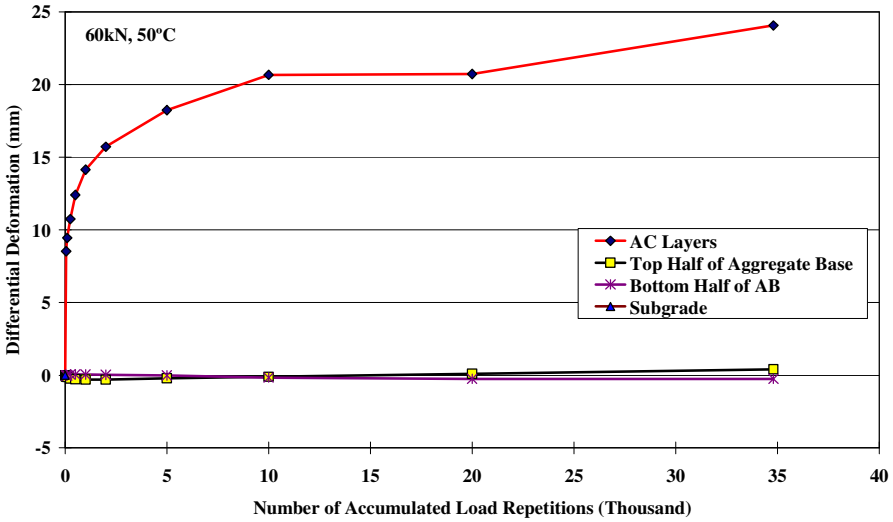

Figure 3.56: 584RF: In-depth differential deformation at MDD8.

3.7.8 Visual Inspection

Apart from rutting, no other distress was recorded on the section. Figure 3.57 shows photographs taken of the surface at the end of the test.

Figure 3.57: 584RF: Section photographs at the end of the test.

3.8. Section 585RF: 45 mm MAC15-G

3.8.1 Test Summary

Loading commenced on October 10, 2003 and ended on October 20, 2003. During this period 3,000 load repetitions were applied and nine datasets were collected.

3.8.2 Air Temperatures in the Temperature Control Unit

Air temperatures inside the temperature control chamber ranged from 35°C to 60°C with an average of 51°C and standard deviation of 4.5°C. Air temperatures were adjusted to maintain a pavement temperature of 50°C±4°C.

The daily average air temperatures recorded in the temperature control unit, calculated from the hourly temperatures recorded during HVS operation, are shown in Figure 3.58. Vertical errors bars on each point on the graph show daily temperature range.

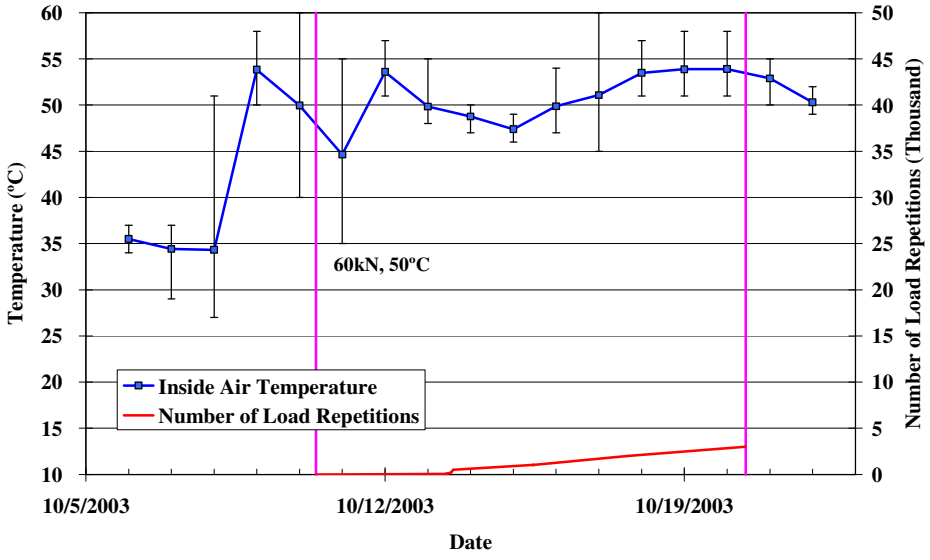

Figure 3.58: 585RF: Daily average air temperatures inside the temperature control chamber.

3.8.3 Outside Air Temperatures

Outside air temperatures ranged from 9°C to 28°C with an average of 15°C and are summarized in Figure 3.59. Vertical error bars on each point on the graph show daily temperature range.

3.8.4 Temperatures in the Asphalt Concrete Layer

Daily averages of the surface and in-depth temperatures are listed in Table 3.16 and shown in Figure 3.60. Pavement temperatures decreased slightly with increasing depth in the pavement.

Table 3.16: 585RF: Temperature Summary for Air and Pavement.

Temperature	Average (°C)	Std Dev (°C)
Outside air	15.3	4.2
Inside air	50.6	4.5
Pavement surface	51.7	3.9
- 25 mm below surface	50.8	3.2
- 50 mm below surface	49.8	2.8
- 90 mm below surface	49.0	2.5
- 120 mm below surface	48.1	2.3

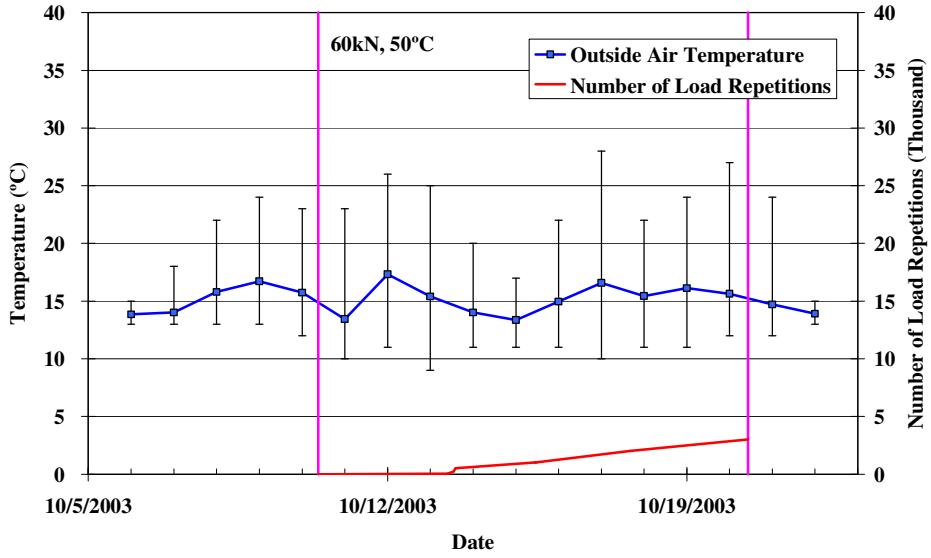

Figure 3.59: 585RF: Daily average air temperatures outside the temperature control chamber.

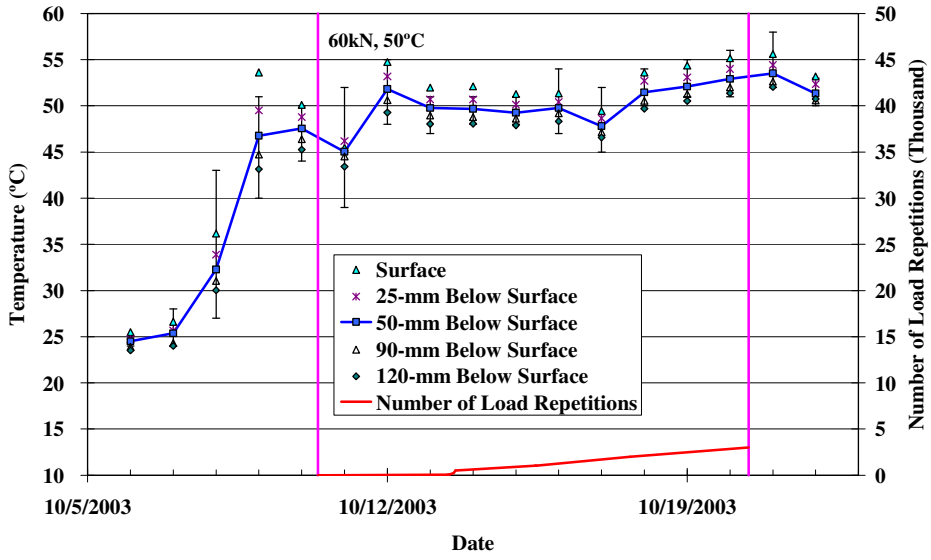

Figure 3.60: 585RF: Daily average temperatures at pavement surface and various depths.

3.8.5 In-depth Elastic Deflection from MDD

In-depth elastic deflection measurements were made with a test load of 60 kN at various times during trafficking. Table 3.17 and Figure 3.61 summarize the in-depth elastic deflections measured at various depths with MDD8.

Table 3.17: 585RF: Summary of 60 kN In-Depth Elastic Deflections.

Depth (mm)	Layer	Elastic Deflection at 60 kN (microns)		
		Before Trafficking	After Trafficking	Ratio of Final/Initial
122	Bottom of underlying DGAC	0.528	0.543	1.03
327	Middle of aggregate base	0.287	0.386	1.34
532	Bottom of aggregate base	0.237	0.302	1.27

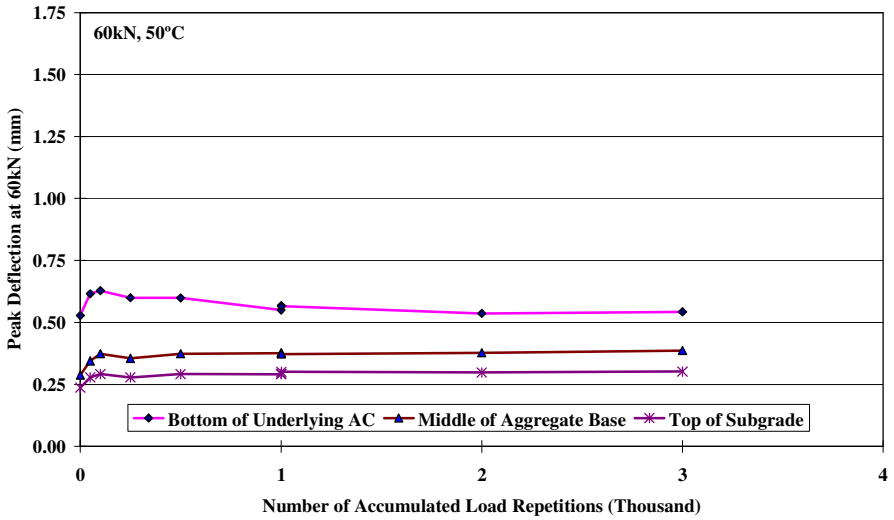

Figure 3.61: 585RF: Elastic deflections at MDD8 with 60 kN test load.

The following observations were made from the data collected:

- The elastic deflections increased slightly at the beginning of the experiment.
- The effect of trafficking load on elastic deformation decreases with increasing depth, as expected. Most of the damage observed appeared to occur in the upper portion of the pavement, which was verified in a forensic investigation (12
- Ratios of final-to-initial MDD deflections show that deflections increased (between 3 and 34 percent) at all depths in the pavement structure by the end of trafficking.

3.8.6 Permanent Surface Deformation (Rutting)

Figure 3.62 shows the average transverse cross section measured with the Laser Profilometer at various stages of the test and clearly shows the increase in rutting and deformation over the duration of the test.

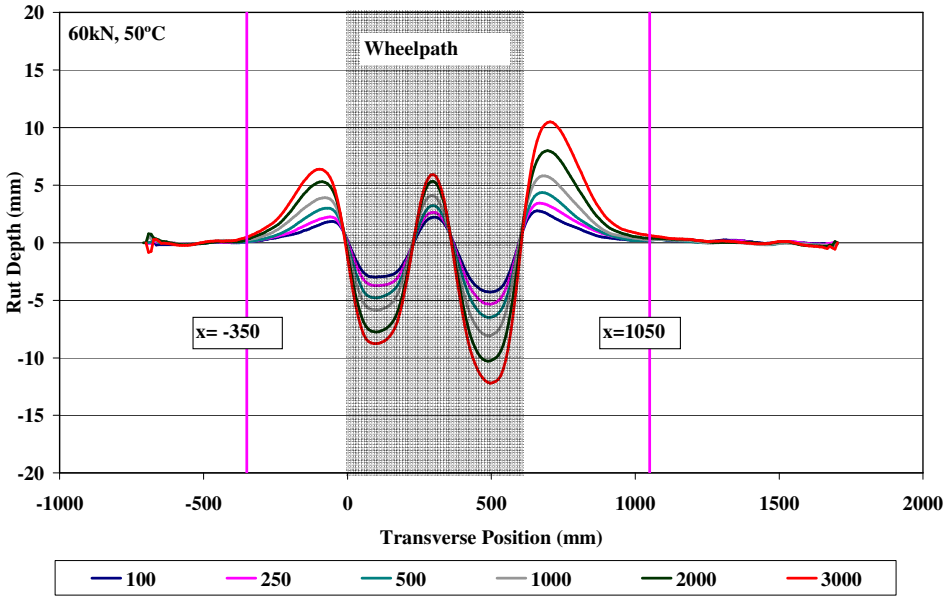

Figure 3.62: 585RF: Profilometer cross section at various load repetitions.

Figures 3.63 and 3.64 show the development of permanent deformation (average maximum rut and average deformation, respectively) with load repetitions as determined by the Laser Profilometer for the test section, with an embedment phase only apparent at the beginning of the experiment. Error bars on the average reading indicate variation along the length of the section. Figure 3.65 shows a contour plot of the pavement surface at the end of the test (3,000 repetitions).

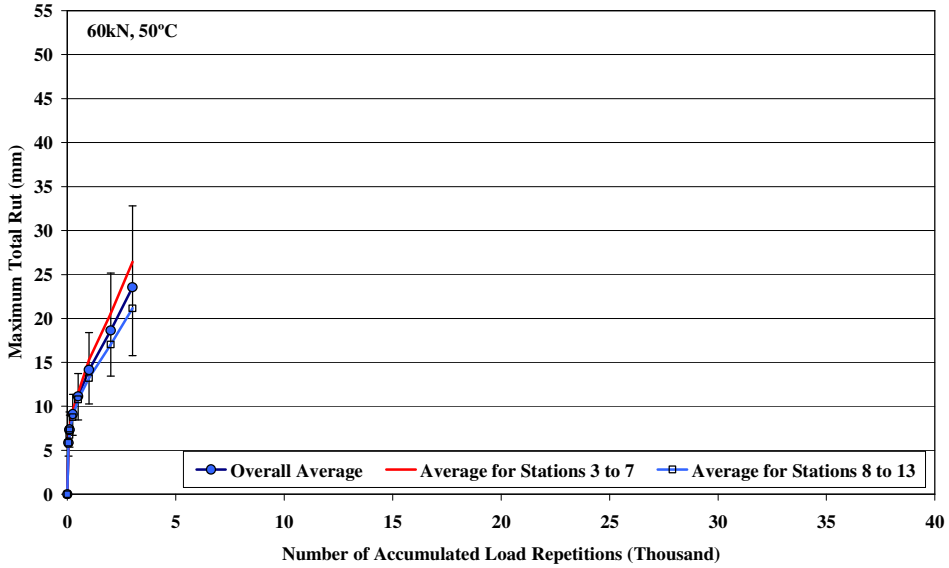

Figure 3.63: 585RF: Average maximum rut.

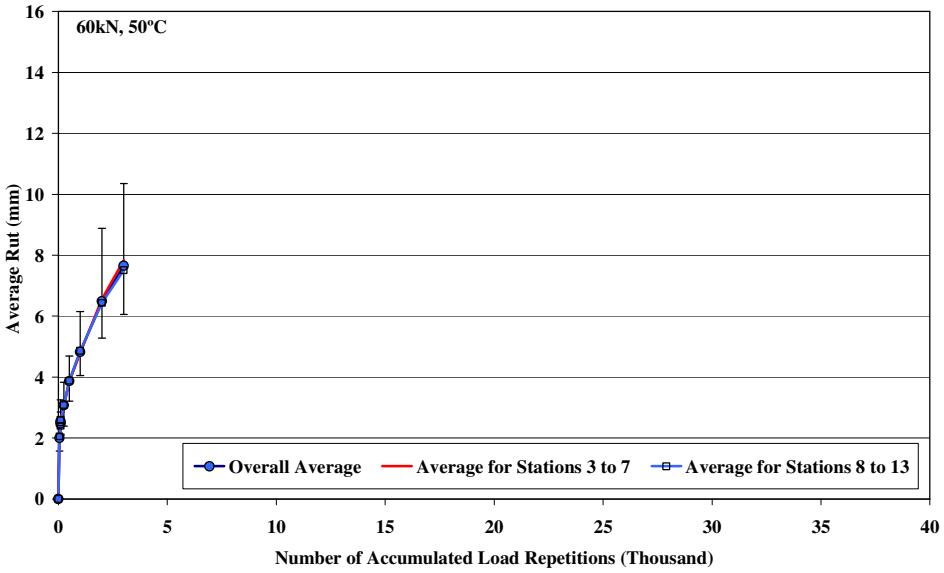

Figure 3.64: 585RF: Average deformation.

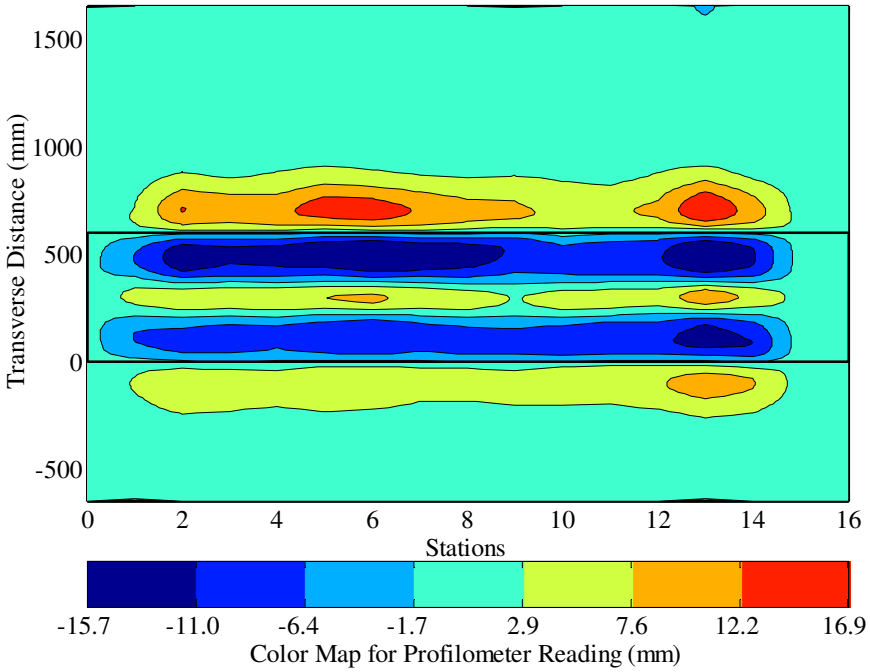

Figure 3.65: 585RF: Contour plot of permanent deformation after 3,000 repetitions.

After completion of trafficking, the average maximum rut depth and the average deformation were 23.5 mm and 7.7 mm, respectively. The maximum rut depth measured on the section was 32.8 mm. Rut development was rapid with the failure criteria of an average of 12.5 mm total rut depth reached after 726 load repetitions.

3.8.7 Permanent In-Depth Deformation

Permanent in-depth deformation was measured with MDD modules installed at Station 8, at the following depths. A module was not installed on the surface of the overlay due to thickness constraints.

- 122 mm: near the bottom of the underlying DGAC layer
- 327 mm: in the middle of the aggregate base layer
- 532 mm: at the bottom of the aggregate base layer
- 722 mm: 300 mm below the top of the subgrade (not functioning in this test)

Table 3.18 and Figures 3.67 and 3.68 provide an indication of the permanent deformation recorded at MDD8. Figure 3.66 shows the permanent deformation at the MDD modules, while Figure 3.67 shows the permanent deformation calculated for the various layers. The data shows that the majority of the permanent deformation occurred in the asphalt concrete layers (93 percent). This was verified in a forensic investigation, which showed that the deformation was almost completely attributable to the underlying DGAC layer (12). No measurable rutting was found in the overlay and approximately 10 mm of shoving occurred at the edges of the trafficked area in the underlying DGAC. Slight differences between the data obtained from the MDDs and the test pit are attributable to the different locations of the MDD and the test pit profile, and the resolution of the profile measurements (~1.0 mm).

Table 3.18: 585RF: Vertical Permanent Deformation in Pavement Layers.

Layer	Nominal Thickness (mm)	Vertical Permanent Deformation (mm)	Percentage Total Deformation (%)
AC layers	135	21.6	93.3
Upper aggregate base	205	1.4	6.1
Lower aggregate base	205	0.1	0.4
Top 300 mm of subgrade	300	<0.1	0.2
Subgrade to anchor	2,158		
Total (All Layers)	3,000	23.1	100

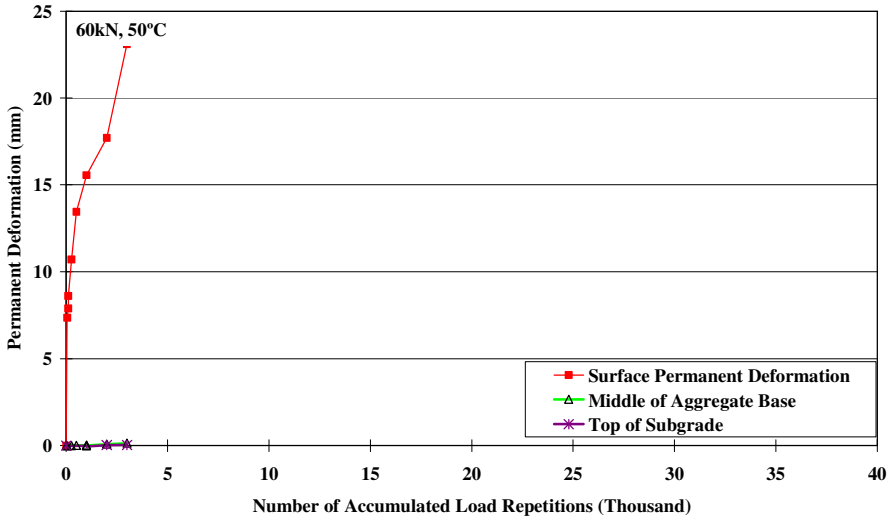

Figure 3.66: 585RF: Permanent in-depth deformation at MDD8.

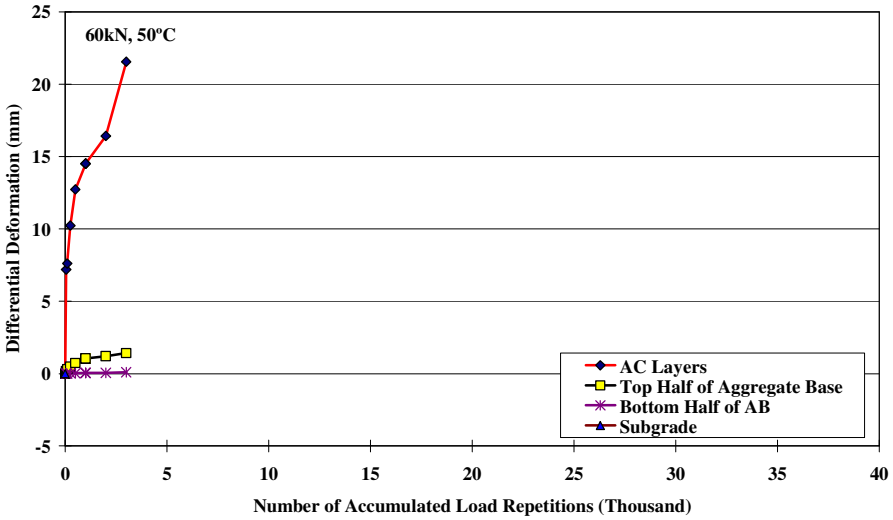

Figure 3.67: 585RF: In-depth differential deformation at MDD8.

3.8.8 Visual Inspection

Apart from rutting, no other distress was recorded on the section. Figure 3.68 shows photographs taken of the surface at the end of the test.

Figure 3.68: 585RF: Section photographs at the end of the test.

3.9. Second-Level Analysis

A second-level analysis report will be prepared on completion of all HVS testing and a forensic evaluation. This report will include:

- Actual layer thicknesses,
- Backcalculation of moduli from MDD and FWD measurements,
- Verification of data collected from in-depth measurements with visual observations from test pits,
- Comparison of performance between test sections,
- Comparisons of HVS test results with laboratory test results;
- Performance modeling and simulations, and
- Recommendations.

4. CONCLUSIONS

This First-Level Report is the seventh in a series of studies detailing the results of HVS testing being performed to validate Caltrans overlay strategies for the rehabilitation of cracked asphalt concrete. It describes the results of the rutting study on HVS sections 580RF through 585RF, carried out on the following overlays:

- Section 580RF: Half-thickness (45-mm) MB4 gap-graded overlay with minimum 15 percent recycled tire rubber (referred to as "MB15-G" in this report);
- Section 581RF: Half-thickness (45-mm) rubberized asphalt concrete gap-graded overlay (RAC-G), included as a control for performance comparison purposes;
- Section 582RF: Full-thickness (90-mm) AR4000 dense graded asphalt concrete (AR4000-D) overlay, included as a control for performance comparison purposes;
- Section 583RF: Half-thickness (45-mm) MB4 gap-graded overlay (45 mm MB4-G);
- Section 584RF: Full-thickness (90-mm) MB4 gap-graded overlay (90 mm MB4-G), and
- Section 585RF: Half-thickness (45-mm) MAC15TR gap-graded overlay with minimum 15 percent recycled tire rubber (referred to as "MAC 15-G" in this report).

The pavement was designed according to the Caltrans Highway Design Manual Chapter 600 using the computer program *NEWCON90*. Design thickness was based on a subgrade R-value of 5 and a Traffic Index of 7 (~121,000 ESALs). The overlay thicknesses were determined according to Caltrans Test Method (CTM) 356 using Falling Weight Deflectometer (FWD) deflections.

HVS trafficking on the sections commenced on September 4, 2003, and was completed on December 16, 2003. During this period, the following load repetitions were applied on each section with a 60 kN (13,500lb) load:

- 580RF (45-mm MB15-G): 2,000 repetitions, equating to 10,980 thousand ESALs
- 581RF (45-mm RAC-G): 7,600 repetitions, equating to 41,725 thousand ESALs
- 582RF (90-mm AR4000-D): 18,564 repetitions, equating to 101,919 thousand ESALs
- 583RF (45-mm MB4-G): 15,000 repetitions, equating to 82,352 thousand ESALs
- 584RF (90-mm MB4-G): 34,800 repetitions, equating to 191,057 thousand ESALs
- 585RF (45-mm MAC15-G): 3,000 repetitions, equating to 16,470 thousand ESALs

A dual tire (720 kPa [104 psi] pressure) and channelized, unidirectional loading was used. A temperature chamber maintained the pavement temperature at 50°C±4°C (122°F±7°F).

Laboratory fatigue and shear studies have been conducted in parallel with HVS testing. Results of these studies are detailed in separate reports. Comparison of the laboratory and test section performance, including the results of a forensic investigation to be conducted when all testing is complete, will be discussed in a second-level report once the data from each of the studies have been collected.

Findings and observations based on the data collected during this HVS study include:

- An aggressive loading regime was followed to induce failure.
- The average maximum rut depths, average maximum deformations, and the number of load repetitions to an average maximum rut depth of 12.5 mm (0.5 in) across each entire test section are summarized in Table 4.1 and shown in Figure 4.1. The sections are ranked from best to worst in terms of rutting performance based on the number of repetitions to reach an average maximum rut depth of 12.5 mm. The reader is reminded that most damage occurred in the underlying DGAC layer.

Table 4.1: Summary of Ranked Rutting Performance.

Rank	Section	Overlay	Average Max. Rut (mm) [in]	Average Deformation (mm) [in]	Max. Rut Depth (mm) [in]	Reps to Failure
1	582RF	AR4000-D	18.8 [0.8]	7.1 [0.3]	20.0 [0.8]	8,266
2	583RF	MB4-G	22.7 [0.9]	10.3 [0.4]	54.3 [2.2]	3,043
3	581RF	RAC-G	15.6 [0.6]	8.1 [0.3]	27.6 [1.1]	2,324
4	584RF	MB4-G	31.3 [1.3]	9.7 [0.4]	29.7 [1.2]	1,522
5	580RF	MB15-G	23.3 [0.9]	11.9 [0.5]	22.3 [0.9]	914
6	585RF	MAC15-G	23.5 [0.9]	7.7 [0.3]	32.8 [1.3]	726

- The AR4000-D and two MB4-G overlays showed a decrease in the rate of rut development just prior to reaching the failure criteria.
- Analysis of surface profiles and test pit observations during the forensic investigation indicate that most of the permanent deformation occurred in the underlying DGAC surfacing layer. The deformation along each section was reasonably uniform, with the exception of Section 584RF, where an area of more severe rutting and heaving occurred at one end of the test section. All of the sections showed some heaving at the sides of the trafficked area, with heights varying between 5.0 and 16 mm (0.2 and 0.6 in).
- The amount of deformation in the asphalt concrete layers as measured by the MDD modules was in general agreement with the observations and measurements from a subsequent forensic investigation.

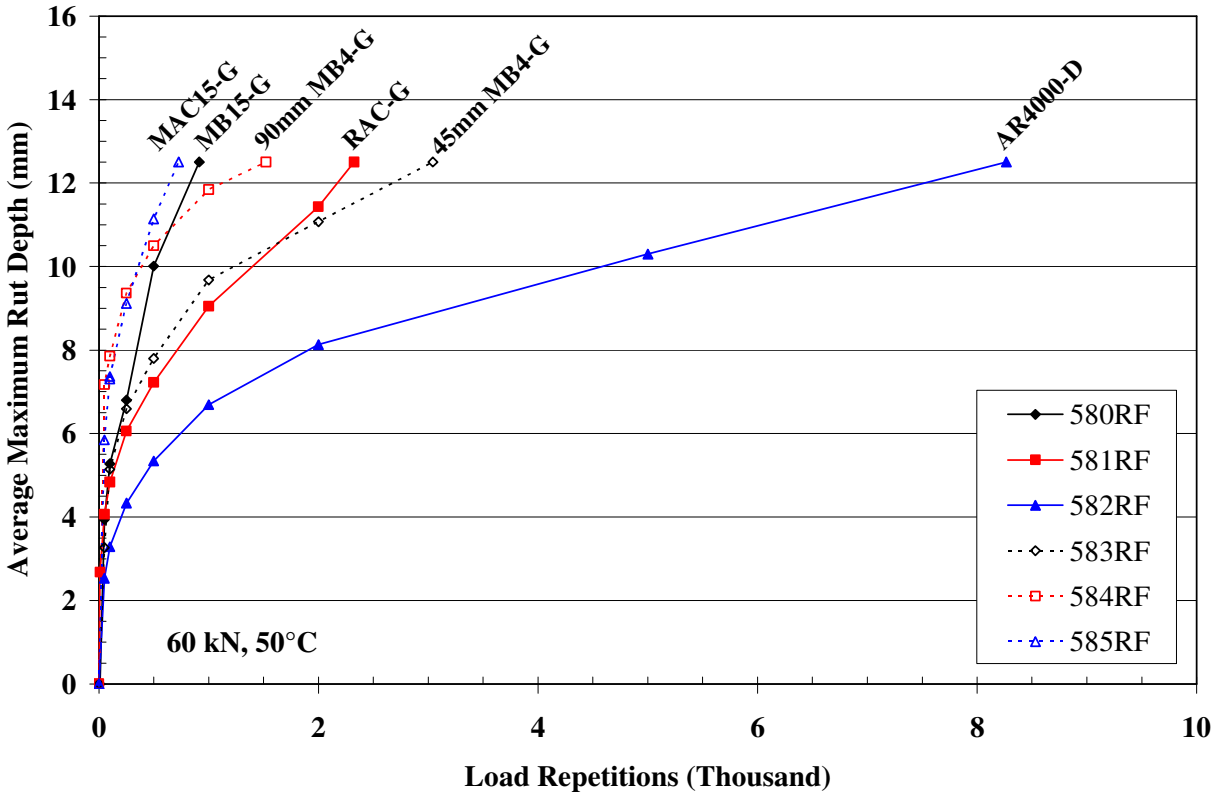

Figure 4.1: Progression of average maximum rut depth to 12.5 mm (0.5 in) failure criteria.

No recommendations as to the use of modified binders in overlay mixes are made at this time. These recommendations will be included in the second-level analysis report, which will be prepared and submitted on completion of all HVS and laboratory testing.

5. REFERENCES

1. **Generic experimental design for product/strategy evaluation — crumb rubber modified materials.** 2005. Sacramento, CA: Caltrans.
2. **Reflective Cracking Study: Workplan for the Comparison of MB, RAC-G, and DGAC Mixes Under HVS and Laboratory Testing.** 2003. Davis and Berkeley, CA: University of California Pavement Research Center. (UCPRC-WP-2003-01).
3. JONES, D., Tsai, B. and Harvey, J. 2006. **Reflective cracking study: First-level report on Section 590RF - 90 mm MB4-G Overlay.** Davis and Berkeley, CA: University of California Pavement Research Center. (Report No. UCPRC-RR-2006-04).
4. JONES, D., Wu, R., Lea, J. and Harvey, J. 2006. **Reflective cracking study: First-level report on Section 589RF - 45 mm MB4-G Overlay.** Davis and Berkeley, CA: University of California Pavement Research Center. (Report No. UCPRC-RR-2006-05).
5. WU, R., Jones, D. and Harvey, J. 2006. **Reflective cracking study: First-level report on Section 587RF - 45 mm RAC-G Overlay.** Davis and Berkeley, CA: University of California Pavement Research Center. (Report No. UCPRC-RR-2006-06).
6. JONES, D., Wu, R. and Harvey, J. 2006. **Reflective cracking study: First-level report on Section 588RF - 90 mm AR4000-D Overlay.** Davis and Berkeley, CA: University of California Pavement Research Center. (Report No. UCPRC-RR-2006-07).
7. JONES, D., Wu, R. and Harvey, J. 2006. **Reflective cracking study: First-level report on Section 586RF - 45 mm MB15-G Overlay.** Davis and Berkeley, CA: University of California Pavement Research Center. (Report No. UCPRC-RR-2006-12).
8. JONES, D., Wu, R. and Harvey, J. 2007. **Reflective cracking study: First-level report on Section 591RF - 45 mm MAC15-G Overlay.** Davis and Berkeley, CA: University of California Pavement Research Center. (Report No. UCPRC-RR-2007-04).
9. HARVEY, J., Du Plessis, L., Long, F., Deacon, J., Guada, I., Hung, D. and Scheffy, C. 1997. **CAL/APT Program: Test Results from Accelerated Pavement Test on Pavement Structure Containing Asphalt Treated Permeable Base (ATPB) – Section 500RF**. Davis and Berkeley, CA: University of California Pavement Research Center. (Report Numbers UCPRC-RR-1999-02 and RTA-65W4845-3).
10. BEJARANO, M., Jones, D., Morton, B., and Scheffy, C. 2005. **Reflective Cracking Study: Summary of Construction Activities, Phase 1 HVS Testing, and Overlay Construction**. Davis and Berkeley, CA: University of California Pavement Research Center. (UCPRC-RR-2005-03).

11. HARVEY, J., Du Plessis, L., Long, F., Deacon, J., Guada, I., Hung, D. and Scheffy, C. 1997. **CAL/APT Program: Test Results from Accelerated Pavement Test on Pavement Structure Containing Untreated Base – Section 501RF.** Davis and Berkeley, CA: University of California Pavement Research Center. (Report Numbers UCPRC-RR-1997-03 and RTA-65W4845-3).

12. JONES, D., Steven, B. and Harvey, J. 2007. **Reflective cracking study: HVS Test Section Forensic Investigation.** Davis and Berkeley, CA: University of California Pavement Research Center. (Report No. UCPRC-RR-2007-05).